

# DISTANCES, AGES AND EPOCH OF FORMATION OF GLOBULAR CLUSTERS <sup>1</sup>

Eugenio Carretta and Raffaele G. Gratton

Osservatorio Astronomico di Padova, Vicolo dell'Osservatorio 5, 35122 Padova, ITALY

carretta@pdmida.pd.astro.it and gratton@pdmida.pd.astro.it

Gisella Clementini and Flavio Fusi Pecci <sup>2</sup>

Osservatorio Astronomico di Bologna, Via Ranzani 1, 40127 Bologna, ITALY

gisella@astbo3.bo.astro.it and flavio@astbo3.bo.astro.it

Received \_\_\_\_\_; accepted \_\_\_\_\_

---

<sup>1</sup>Based on data from the Hipparcos astrometry satellite

<sup>2</sup>Also Stazione Astronomica, 09012 Capoterra, Cagliari, ITALY

## ABSTRACT

We review the results on distances and *absolute* ages of galactic globular clusters (GCs) obtained after the release of the Hipparcos catalogue. Several methods aimed at the definition of the Population II local distance scale are discussed, and their results compared, exploiting new results for RR Lyraes in the Large Magellanic Cloud (LMC). We find that the so-called *Short* and *Long* Distance Scales may be reconciled whether a consistent reddening scale is adopted for Cepheids and RR Lyrae variables in the LMC .

Emphasis is given in the paper to the discussion of distances and ages of GCs derived using Hipparcos parallaxes of local subdwarfs. We find that the selection criteria adopted to choose the local subdwarfs, as well as the size of the corrections applied to existing systematic biases, are the main culprit for the differences found among the various independent studies that first used Hipparcos parallaxes and the subdwarf fitting technique. We also caution that the absolute age of M92 (usually considered one of the oldest clusters) still remains uncertain due to the lack of subdwarfs of comparable metallicity with accurate parallaxes.

Distances and ages for the 9 clusters discussed in Paper I are re-derived using an enlarged sample of local subdwarfs, which includes about 90% of the metal-poor dwarfs with accurate parallaxes ( $\Delta\pi/\pi \leq 0.12$ ) in the whole Hipparcos catalogue. On average, our revised distance moduli are decreased by 0.04 mag with respect to Paper I. The corresponding age of the GCs is  $t = 11.5 \pm 2.6$  Gyr, where the error bars refer to the 95% confidence range. The relation between zero age horizontal branch (ZAHB) absolute magnitude and metallicity for the nine programme clusters turns out to be  $M_V(ZAHB) = (0.18 \pm 0.09)([Fe/H] + 1.5) + (0.53 \pm 0.12)$  Thanks to Hipparcos

the major contribution to the total error budget associated with the subdwarf fitting technique has been moved from parallaxes to photometric calibrations, reddening and metallicity scale. This total uncertainty still amounts to about  $\pm 0.12$  mag.

We then compare the corresponding (true) LMC distance modulus  $\mu_{\text{LMC}} = 18.64 \pm 0.12$  mag with other existing determinations. We conclude that at present the best estimate for the distance of the LMC is:

$$\mu_{\text{LMC}} = 18.54 \pm 0.03 \pm 0.06$$

suggesting that distances from the subdwarf fitting method are  $\sim 1 \sigma$  too long. Consequently, our best estimate for the age of the GCs is revised to:

$$\text{Age} = 12.9 \pm 2.9 \text{ Gyr}$$

(95% confidence range). The best relation between ZAHB absolute magnitude and metallicity is:

$$M_V(\text{ZAHB}) = (0.18 \pm 0.09)([\text{Fe}/\text{H}] + 1.5) + (0.63 \pm 0.07)$$

Finally, we compare the ages of the GCs with the cosmic star formation rate recently determined by studies of the Hubble Deep Field, exploiting the determinations of  $\Omega_M = 0.3$  and  $\Omega_\Lambda = 0.7$  provided by type Ia SNe surveys. We find that the epoch of formation of the GCs (at  $z \sim 3$ ) well matches the maximum of the star formation rate (SFR) for elliptical galaxies in the HDF as determined by Franceschini et al. (1998).

*Subject headings:* Clusters: globulars – Cosmology – Stars: basic parameters – Stars: stellar models – The Galaxy: evolution of

## 1. INTRODUCTION

In the last two years, new important sets of data have allowed for the first time to connect the epoch of formation of local fossil remnants with evidences from the remote Universe:

- The global history of star formation is now beginning to be reconstructed, mainly thanks to data provided by the Canada-France Redshift Survey (Lilly et al. 1996) and the Hubble Deep Field (HDF: Madau et al. 1996; Madau, Pozzetti & Dickinson 1998). Although quite large uncertainties still exists, mainly related to the role of dust, these data robustly locate the bulk of cosmic star formation at  $z \geq 1$ ; for spheroidal systems, it is at  $z \sim 2 - 3$  (Franceschini et al. 1998).
- Two independent, broad impact surveys of moderately high redshift type Ia SNe (Schmidt et al. 1998; Perlmutter et al. 1998) coupled to constraints from Cosmic Microwave Background (Garnavich et al. 1998; Lasenby 1998) have yielded very precise values for  $\Omega_M \sim 0.3 \pm 0.1$  and  $\Omega_\Lambda \sim 0.7 \pm 0.1$ . Note that these small error bars are obtained assuming a flat Universe. If confirmed, this very exciting result will allow a much better definition of the Universe geometry than possible insofar
- The ESA HIPPARCOS satellite has provided new, much more accurate values for the trigonometric parallaxes of  $\sim 118,000$  nearby stars, including a rather large number of Cepheids, horizontal branch stars, and subdwarfs. This has allowed reliable estimates of distances and ages for the LMC and the globular clusters (GC: Feast & Catchpole 1997; Reid 1997, 1998; Gratton et al. 1997a; Pont et al. 1998; Madore & Freedman, 1998; Fernley et al. 1998a; Chaboyer et al. 1998; Grundahl et al. 1998)
- New data sets for variables in the LMC, from microlensing experiments (MACHO, EROS, OGLE), as well as from other observing programs (Walker 1992; Clementini

et al. 2000) have allowed to clarify critical issues like the rôle of reddening in distance derivations to this very important galaxy

The combined impact of these works is enormous, since first it allows to reconcile the ages of GCs with the present and past expansion rate of the Universe, and second opens new perspectives on galactic evolution studies. In the present paper we re-examine the current status of knowledge about distances and ages for GCs and discuss their impact on the cosmic distance scale. Finally, we sketch the present evidences about the epoch of formation of galactic GCs (assumed to be tracers of the earliest epoch of star formation in our own Galaxy), comparing it with the current knowledge about the cosmic star formation history.

## 2. SHORT AND LONG DISTANCE SCALES AND THEIR IMPLICATIONS

The status of the research on the absolute age of GCs, and its impact on the choice of a cosmological model for the Universe, is summarized in Figure 1, adapted and updated from Turner (1997).

As well known, the main problem in the derivation of ages for GCs is the unambiguous definition of a reliable distance scale for population II stars (Renzini, 1991), since a marked dichotomy exists insofar between a **long distance scale** and a **short distance scale** (see Vandenberg, Bolte & Stetson 1996). Indeed, once the distance is fixed, absolute ages for the GCs can be derived from the absolute magnitude of their turn off,  $M_V(TO)$ , which is the evolutionary "clock".

Depending on which distance scale is adopted, a rather striking impact follows on the cosmological framework. In fact, if the short distance scale is adopted, the HB luminosity

would be  $M_V(HB) \sim 0.75$  at  $[\text{Fe}/\text{H}] \simeq -1.5$ , GC absolute ages would be  $\sim 16$  Gyr<sup>3</sup>, and a distance modulus of  $\mu_{\text{LMC}} \sim 18.25$  would be derived for the LMC. This value is 0.25 mag smaller than that adopted in extragalactic distance scales (e.g. the HST Key Project on Extragalactic Cepheids), and implies a value for  $H_0$  roughly in the range 65–85 km s<sup>−1</sup>Mpc<sup>−1</sup> (this residual range being mainly due to ambiguities in the location of spiral galaxies within the Virgo cluster: Tammann 1998). On the other side, if the long distance scale is adopted, the HB luminosity would be  $M_V(HB) \sim 0.5$  at  $[\text{Fe}/\text{H}] \simeq -1.5$ , GC's ages would be  $\sim 13$  Gyr, and the distance modulus to the LMC would be  $\mu_{\text{LMC}} \sim 18.5$ , consistent with  $H_0$  roughly in the range 55–75 km s<sup>−1</sup>Mpc<sup>−1</sup>.

For this reason, Figure 1 is divided in two panels. In Panel *a* we compared the age of GC derived before data from the Hipparcos mission became available (Bolte & Hogan 1995, Chaboyer et al. 1996; VandenBerg et al. 1996), with the age of a (flat) Universe provided by different values of  $H_0$ , for different values of  $\Omega_\Lambda = 1 - \Omega_M$ , and within the range indicated by the recent type Ia SNe data ( $\Omega_M \sim 0.3 \pm 0.1$ ). The shaded region is the permitted area, obtained adopting values of  $H_0$  consistent with the distance moduli used to derive the ages for the GCs. While the rather large error bars indeed allow some region of overlap, strong constraints are required for the epoch of formation of the GCs.

The advent of Hipparcos parallaxes has allowed to greatly improve one of the most powerful (but up to now uncertain due to the lack of a proper data base) method to derive distances: the GC subdwarf fitting technique. It will be shown that once questions related to a correct handling of the data sample are properly addressed, this method favours the "long distance scale", and the derivation of younger ages for GCs. As shown in panel *b* of Figure 1, the derived ages are now comfortably smaller than the age of the Universe.

---

<sup>3</sup>For M92, the age derived using the short distance scale would be as large as  $\sim 18.5$  Gyr

While the distance scale provided by the subdwarf fitting method agrees with the most accurate and up-to-now robust distance indicator: the Cepheids, it must be emphasized that, so far, other recent results did not easily fit into this reassuring and consistent picture. In fact, a number of distance scale determinations still support the short distance scale. For instance, Hipparcos proper motions for the field RR Lyraes have confirmed the results obtained by ground-based statistical parallaxes. However, in the following we will show that once reddening for the RR Lyraes in the LMC are assumed consistently with those used for the LMC Cepheids, this dichotomy is solved. This result is new and will be discussed in some depth in the next Section.

### 3. DISTANCES TO POPULATION II OBJECTS. A REVIEW

Globular clusters, as well as most of the Population II objects, are too far to allow a direct measure of their trigonometric parallaxes with the presently available instrumental tools. Therefore, several *indirect* techniques have been devised, in order to measure their distances. Some of them exploit the classical *standard candles* existing among Pop. II objects (red giant branch - RGB - stars, horizontal branch - HB - stars, RR Lyrae variables, main sequence - MS - subdwarfs, white dwarfs - WD), others follow alternative approaches. In this Section, we will consider several of these distance indicators, both from population II and (for comparison) from population I objects. We will postpone a thorough discussion of distances obtained via main sequence fitting to the next Section. Also, we will not consider distances derived from calibration of luminosities entirely based on models (like e.g. stellar or pulsational models). While most of the results we find here agree with the model predictions, we prefer to keep results mainly based on observations clearly separated from results entirely based on model calculations. In this way, first, the results will not critically depend on the model assumptions, and, second, they may be used to test the

model predictions (see e.g. Gratton, 1998c; Castellani, 1999). On the other hand, ages for clusters cannot be derived without reference to models: however, the adopted calibrator - the MS turn-off luminosity - is a very robust theoretical prediction.

The various distance indicators will be discussed through the comparison of the values for the (true) distance modulus of the LMC,  $\mu_{\text{LMC}}$ , they lead to. When considering distances to the LMC derived from population II objects the following two issues should be reminded :

- Distances to the LMC are finally founded on the RR Lyrae variables. The absolute magnitude of RR Lyrae is known to depend on metallicity, but there is no general agreement about the correct slope  $dM_V(RR)/d[\text{Fe}/\text{H}]$  of the absolute magnitude-metallicity relation. In the following, we will assume a value of  $dM_V(RR)/d[\text{Fe}/\text{H}] = 0.18 \pm 0.09$ , which is supported by most theoretical models (Chieffi, Straniero & Limongi, 1998, Caloi, D'Antona & Mazzitelli 1997, Cassisi et al. 1997, VandenBerg, 1997), and Baade-Wesselink absolute magnitudes (Fernley et al. 1998b), and it is only slightly larger than derived from the GCs in M31 (Fusi Pecci et al. 1996). Both models and observations suggests that the relation is probably steeper at metallicity  $[\text{Fe}/\text{H}] > -1$  (however, this range is not relevant for the present discussion). Anyway, the impact of this source of uncertainty ( $< \pm 0.1$  mag/dex) on our discussion is small. In fact, our choice was to refer our absolute magnitude estimates to a metallicity of  $[\text{Fe}/\text{H}] = -1.5$ , that is a typical average value for most of the population II distance indicators: for instance, the average for our nine globular clusters is  $[\text{Fe}/\text{H}] = -1.42$ , that for HB stars with Hipparcos parallaxes considered by Gratton (1998b, see below) is  $-1.41$ , and that for the RR Lyrae used in the statistical parallaxes ranges from  $-1.53$  to  $-1.61$ , depending on the adopted sample. We argue that also RR Lyrae in the bar of the LMC have on average a similar metallicity, albeit

evidence is admittedly not as strong as desired. However, on the whole we think that uncertainties related to these transformations are *on average*  $< \pm 0.02$  mag, and cannot explain significant parts of the discrepancy between the short and long distance scale, while of course they may be important for individual clusters at the extremes of the metallicity range like M92 or 47 Tuc (in these cases, uncertainties in the distances may be as large as  $\sim 0.07$  mag, corresponding to  $\sim 1$  Gyr)

- Clementini et al. 1999 have recently derived an average magnitude of  $V = 19.33 \pm 0.02$  for 75 RR Lyraes in two fields of the bar of the LMC<sup>4</sup>. They compare this value, which is assumed to correspond to an average metal abundance  $[\text{Fe}/\text{H}] = -1.5$  dex (from the  $\Delta S$  analysis of a sample of double-mode pulsators in the LMC), with Walker (1992) average dereddened magnitude of the cluster RR Lyraes :  $< V_0 > = 18.94 \pm 0.04$  mag (at an average metallicity of  $[\text{Fe}/\text{H}] = -1.9$  and for an average reddening  $E(B-V) \sim 0.09$  mag). On the assumption of a reddening value  $E(B-V) = 0.10$  mag for the LMC bar (Bessel, 1991) they conclude that (i) the two  $< V_0 >$  estimates are in very good agreement once the 0.4 dex difference in metal abundance is accounted for (with a slope of 0.18 for the metallicity-luminosity relation for HB stars), and that (ii) no evidence is found for a difference in luminosity between field and cluster RR Lyraes in the LMC. When combined with the faint absolute magnitudes given by e.g. statistical parallaxes, these  $< V_0 >$  values for the RR Lyrae's in LMC produce the so called *short distance scale*.

In a separate paper, (Clementini et al. 2000, in preparation), we present a detailed

---

<sup>4</sup>This value is close to that estimated by the MACHO experiment (Alcock et al. 1996), however, the band width used by MACHO is quite different from the standard Johnson system, so that Alcock et al.'s color corrections are more uncertain than in Clementini et al. photometry

description of this new LMC RR Lyrae data set and discuss several determinations of reddening towards the bar of the LMC. The (average) value consistent with the analysis of the Cepheids (Caldwell & Coulson 1985, Laney & Stobie 1993, Gieren, Fouqué & Gomez 1998) is  $E(B - V) = 0.07$ ; while a slightly larger value of  $E(B - V) = 0.09$  would give colors of the edges of the instability strip consistent with those found for the LMC GCs (Walker 1992). Finally, an even larger value :  $E(B - V) = 0.13$  is given by the reddening maps of Schlegel, Finkbeiner & Davis (1998), Oestreicher, Gochermann & Schmidt-Kaler (1995) and Oestreicher & Schmidt-Kaler (1996)<sup>5</sup>. This range in the reddening value obtained for the same locations within the LMC is large, and may explain most of the scatter in the recent determinations of the distance modulus of the LMC. In fact, the reddening value used by Walker (1992), as well as Bessel's (1991), are on average  $\sim 0.02$ - $0.03$  mag larger than values consistent with the Cepheids analysis. Once corrected for this effect, GC RR Lyraes are on average  $0.03 \pm 0.05$  mag brighter than the field RR Lyraes, a difference entirely due to a single cluster (NGC 1841), that is likely to be  $\sim 0.2$  mag closer to us than the LMC (Walker 1992).

Hereinafter, we will adopt the reddening scale given by Cepheids (0.07 mag) which is also supported by a comparison of the colors of the edges of the instability strip for the field LMC RR Lyraes with those defined by variables in the globular cluster M3 (Clementini et al. 2000). A major advantage of this choice is that it allows a consistent comparison of distance scales from population I and II indicators; this is one of the main tools of our analysis. With this reddening value **we obtain an average**

---

<sup>5</sup>When deriving reddening values from these maps, we added the foreground reddening and half of the internal reddening, under the assumption that half of the variables are in front of the absorbing layer, and half behind it.

**magnitude for RR Lyraes in the bar of the LMC of**  $\langle V_0 \rangle = 19.11 \pm 0.02$ . The average metallicity of the bar RR Lyraes is not well determined. In the following, we will assume a value of  $[\text{Fe}/\text{H}] = -1.5 \pm 0.2$ , as the combination of Alcock et al. (1996, 1997) estimates, and of the  $\Delta S$  metal abundances for a sample of LMC double-mode pulsators (Bragaglia et al. 2000, in preparation).

### 3.1. Population II distance indicators

#### a) *RR Lyrae and HB stars. Trigonometric Parallaxes*

Gratton (1998b) found that the average absolute magnitude of a sample of 22 field metal-poor HB stars with trigonometric parallaxes measured by Hipparcos is  $M_V = +0.69 \pm 0.10$  (at average metallicity  $[\text{Fe}/\text{H}] = -1.41$ ). Popowski & Gould (1998b) reanalyzed Gratton's (1998b) HB sample, and after elimination of all the red HB stars, because they may be contaminated by RGB stars, they derive  $M_V = +0.69 \pm 0.15$  (at average metallicity  $[\text{Fe}/\text{H}] = -1.62$ ). While the revision by Popowski & Gould may be questionable since the metallicity scale for BHB stars is not well determined, Koen & Laney (1998) have shown that the distances derived by Gratton (1998b) are slightly underestimated because the intrinsic scatter in HB magnitudes was neglected when correcting for the Lutz-Kelker effect. The revised relation for RR Lyrae magnitude from trigonometric parallaxes of HB stars is then:

$$M_V(RR) = 0.18([\text{Fe}/\text{H}] + 1.5) + 0.62 \pm 0.11.$$

The corresponding distance modulus for the LMC is:

$$\mu_{\text{LMC}} = 18.49 \pm 0.11$$

#### b) *RR Lyrae and HB stars. Statistical Parallaxes*

The Statistical Parallax method applied to galactic field RR Lyraes leads to a faint zero-point of the RR Lyrae luminosity calibration. Using ground-based proper motions, Layden et al. (1996) obtained  $M_V = 0.71 \pm 0.12$  at  $[\text{Fe}/\text{H}] = -1.61$ . More recently, Popowski & Gould (1998a) have re-analyzed Layden et al.'s sample essentially confirming their results. The Hipparcos based Statistical Parallax analysis by Fernley et al. (1998a) and Tsujimoto, Miyamoto & Yoshii (1997), also give a faint absolute magnitude. These different estimates are well consistent to each other. However, since they use very similar techniques and often the same observational data base, the error bar of the average is essentially the same as that of the individual determinations. A reasonable summary of these different results yields then the following relation for RR Lyrae absolute magnitude:

$$M_V(RR) = 0.18([\text{Fe}/\text{H}] + 1.5) + 0.73 \pm 0.12.$$

The corresponding distance modulus for the LMC is:

$$\mu_{\text{LMC}} = 18.38 \pm 0.12$$

c) *RR Lyrae and HB stars. The Baade-Wesselink method.*

The Baade-Wesselink (B-W) method (Baade, 1926; Wesselink, 1969) uses the color, light and radial velocity variations of an RR Lyrae variable during the pulsation cycle, to derive its distance and absolute luminosity. This technique in its two major variants, the surface brightness and the infrared flux method (see Cacciari, Clementini & Fernley 1992, and references therein), has been applied to about 30 field's and to a few cluster variables (Liu & Janes 1990a,b, Jones et al. 1992, Cacciari et al. 1992, Skillen et al. 1993, Storm, Carney & Latham 1994), leading to a relatively mild slope of the  $M_V, [\text{Fe}/\text{H}]$  relation, (as opposite to the steep slope of 0.30 found by Sandage, 1993) and to a zero-point similar to that provided by statistical parallaxes. Several attempts have been made to reconcile the B-W results with the Cepheids distance scale. Fernley (1994) proposes a different value

of the conversion factor ( $p$ ) between observed and true pulsation velocity, thus getting a zero-point of the  $M_V, [\text{Fe}/\text{H}]$  relation 0.07 mag brighter than in classical B-W analyses (see also Clementini et al. 1995). However, this only accounts for about 1/3 of the original discrepancy. Feast (1997), using a compilation of B-W literature data and adopting  $M_V$  as independent variable, derives  $M_V = 0.37[\text{Fe}/\text{H}] + 1.13$ . When combined with Walker (1992) data for the RR Lyraes in the LMC, this calibration provides  $\mu_{\text{LMC}} = 18.52$ , in agreement with the classical modulus from Cepheids. However, Feast procedure is rather questionable, since it attributes zero error to  $M_V$ , which is by far the most uncertain quantity of the  $M_V, [\text{Fe}/\text{H}]$  relation.

A revision of the B-W results based on the assumption that optical and near-infrared colors are better temperature indicators than the  $V - K$  index, is proposed by McNamara (1997). When applied to the RR Lyraes in the LMC, this calibration gives  $\mu_{\text{LMC}} = 18.54 \pm 0.10$ . However, systematic errors are likely to affect McNamara procedure, since inconsistently derived quantities are used.

Summarizing, the Baade-Wesselink method favours the following calibration for the RR Lyrae magnitudes:

$$M_V(RR) = 0.18([\text{Fe}/\text{H}] + 1.5) + 0.71 \pm 0.08.$$

(Clementini et al. 1995). The corresponding distance modulus for the LMC is:

$$\mu_{\text{LMC}} = 18.40 \pm 0.08 \pm 0.2,$$

where the first error bar is the internal one. However, given the theoretical uncertainties related to the method, a more realistic error bar is perhaps  $\sim 0.2$  (Jones et al. 1992). This is the error we will adopt in our discussion.

d) *RR Lyrae and HB stars. Double-mode RR Lyraes*

Thanks to the large amount of data from the MACHO experiment, Alcock et al. (1997) were able to identify 73 double-mode RR Lyraes (RRd) near the bar of the LMC. In these stars the ratio of the fundamental-to-first-overtone period allows an accurate estimate of the star mass; they can thus be used to derive pulsation-based luminosities of the HB. Alcock et al. assumed that their variables are at Fundamental Blue Edge (FBE) of the instability strip and then using the  $P_{\text{FBE}}$ -[Fe/H] and  $\log T_{\text{eff}}$ -[Fe/H] relations by Sandage (1993), obtain a calibration of the RR Lyrae luminosity with a bright zero-point. This calibration leads to a distance modulus of the LMC of:

$$\mu_{\text{LMC}} = 18.48 \pm 0.19,$$

for an assumed mean reddening of  $E(B - V) = 0.086$ . This reddening is slightly larger than the value used for Cepheids, so the comparison is somewhat uncertain. However, since this source of uncertainty is much smaller than the internal error bar of the determination, we may neglect it in our discussion.

e) *Dynamical models for globular clusters*

Astrometric distances to GCs can be derived from the comparison of proper motion and radial velocity dispersion within each cluster, using King-Michie type dynamical models (Rees, 1996). The method does not make use of *standard candles* and is independent of stellar evolution models. However, since results for individual clusters may be affected by large error bars, and depend on cluster dynamical models (e.g. the incidence of binaries and the presence of rotation), a large number of clusters should be analyzed in order to increase the accuracy of the method. Rees (1996) derives distances based on this technique for ten GCs. However, some of the analyzed clusters have rather uncertain data. Chaboyer et al. (1998) restrict Rees' analysis to the 6 clusters with most reliable data, getting  $M_V(RR) = 0.59 \pm 0.11$  at  $[\text{Fe}/\text{H}] = -1.59$ .

Summarizing, the astrometric distances to GCs yields the following calibration for the

RR Lyrae magnitudes:

$$M_V(RR) = 0.18([\text{Fe}/\text{H}] + 1.5) + 0.61 \pm 0.11.$$

The corresponding distance modulus for the LMC is:

$$\mu_{\text{LMC}} = 18.50 \pm 0.11$$

f) *The White Dwarfs Cooling Sequence*

The distance to a given cluster may be derived from the comparison of its WD cooling sequence with a template sequence formed by local WDs with known parallaxes and masses. This method has the advantage of being independent of metallicity and age as well as of details of the convection theory. WDs have been observed with HST in a number of GCs (M4, Richer et al. 1995;  $\omega$  Cen, Elson, Gilmore & Santiago, 1995; M15, De Marchi & Paresce, 1995; NGC 6397, Cool, Piotto & King, 1996; NGC 6752, Renzini et al. 1996; 47 Tuc, Zoccali et al. 1998). So far, the method has been applied only to NGC 6752 (Renzini et al. 1996), and 47 Tuc (Zoccali et al. 1998).

The derived distances favour the short distance scale, and the following calibration (not explicitly given in the original papers) can be obtained for the RR Lyrae magnitudes:

$$M_V(RR) = 0.18([\text{Fe}/\text{H}] + 1.5) + 0.7 \pm 0.15.$$

The corresponding distance modulus for the LMC is:

$$\mu_{\text{LMC}} = 18.4 \pm 0.15$$

The major shortcomings of this technique are (i) the difficulties in comparing HST colors for objects having very different apparent magnitude, and (ii) the assumption that the calibrating WDs share the same mass as the GC WDs, an assumption that may be

criticized in view of the differences in the age of the parent populations, and of the different techniques used to derive masses for field and cluster WDs. These two effects are quite difficult to be estimated, however our rather large (and subjective) error bars should be adequate to represent them.

### 3.2. Population I distance indicators

Distances to the LMC can be also derived using population I distance indicators. It is very important to compare these distances with those provided by the population II objects.

#### a) *Classical Cepheids. Trigonometric parallaxes*

The Cepheid period-luminosity relation is traditionally the most accurate method to derive distances to nearby galaxies. Feast & Catchpole (1997) have obtained a new P-L relation at V for classical Cepheids:  $\langle M_V \rangle = -2.81 \log P - 1.43$ , where the slope is that obtained by Caldwell & Laney (1991) from 88 Cepheids in the LMC, and the zero-point is based on the Hipparcos parallaxes of a sample of Galactic Cepheids. When combined with an appropriate correction for the metallicity dependence (+0.042 taken from Laney & Stobie, 1994), this relation gives  $\mu_{\text{LMC}} = 18.70 \pm 0.10$ . This result was criticized by various authors (Szabados 1997; Madore & Freedman 1998; Oudmaijer, Groenewegen & Schrijver 1998). However, Pont (1998) in his thorough discussion of all these papers concluded that Feast & Catchpole analysis is unbiased (as demonstrated by appropriate MonteCarlo simulations), although Feast & Catchpole error bar is likely to be underestimated, a more appropriate value being  $\pm 0.16$  mag. The same conclusion has been reached analytically by Koen & Laney (1998).

Summarizing, the Hipparcos based trigonometric parallaxes of Cepheids support a

distance modulus to the bar of the LMC of :

$$\mu_{\text{LMC}} = 18.70 \pm 0.16$$

b) *Classical Cepheids. Main Sequence Fitting*

The zero point of the Period-Luminosity relation for Cepheids can be obtained using Cepheids in clusters. Adopting this technique, Laney & Stobie (1994) obtained a distance modulus of  $\mu_{\text{LMC}} = 18.49 \pm 0.04[\pm 0.04]$  where the former is the internal error, and the latter is the systematic one. As pointed out by Pont (1998), this distance modulus corresponds to a Hyades distance modulus of 3.27, slightly shorter than the very precise determination by Hipparcos ( $3.33 \pm 0.01$ ). Once corrected for this effect, Laney & Stobie (1994) distance to LMC is modified to:

$$\mu_{\text{LMC}} = 18.55 \pm 0.04[\pm 0.04]$$

Possible uncertainties in this determination arise from Hipparcos revised distance modulus for the Pleiades (Mermilliod et al. 1997), that, if adopted, makes the cluster Cepheid P-L relation about 0.3 mag fainter. However, Hipparcos distance modulus for the Pleiades might have an error bar much larger than originally estimated, because all Pleiades stars lie in a small region on the sky (Soderblom et al. 1998; Pinsonneault et al. 1998; Narayanan & Gould 1999); in this case individual parallax determinations cannot be considered as independent, and the error bar should not decrease with the square root of the number of stars. An error bar as large as  $\pm 0.2$  mag may likely be attributed to the Pleiades distance modulus from Hipparcos parallaxes<sup>6</sup>.

c) *Classical Cepheids. Baade-Wesselink Method*

---

<sup>6</sup>According to Narayanan & Gould, errors are much smaller for the Hyades, due to the larger individual parallaxes, and their location on the sky

A further independent approach is followed by Gieren et al. (1998), who used the infrared Barnes-Evans surface brightness technique to derive accurate infrared distances to 34 Galactic Cepheids. These distances were then used to determine period-luminosity relations at various passbands, which are compared to analogous relations for Cepheids in the LMC. On the assumption of the same slope of the PL relation for the Galactic and the LMC Cepheids, Gieren et al. (1998) derive a distance modulus for the LMC of  $\mu_{\text{LMC}} = 18.46 \pm 0.06$ . However, this distance modulus has been obtained with a slope of the Period-Luminosity relation steeper than Caldwell & Laney (1991) one. If the latter is adopted, consistently with the other Cepheids distance determinations, Gieren et al. distance modulus for the LMC becomes:  $\mu_{\text{LMC}} = 18.52 \pm 0.06$ . Using an empirical procedure based on the geometric Baade-Wesselink method calibrated against high-precision data from spectroscopic and interferometric techniques applied to Galactic Cepheids, Di Benedetto (1997) obtained a corrected distance modulus for the LMC of  $\mu_{\text{LMC}} = 18.58 \pm 0.024$ , which agrees well with the (corrected) value of Gieren et al. Note that Di Benedetto used a period-luminosity-color ( $V - K$ ) relation for Cepheids. The slope of this relation cannot be easily compared with the slope of the period-luminosity relation (at  $V$ ) used by Feast & Catchpole. For this reason we prefer to apply no (uncertain) corrections to the value given by Di Benedetto.

Averaging the result by Gieren et al. and Di Benedetto, we conclude that the Baade-Wesselink method for Cepheids yields a distance modulus of:

$$\mu_{\text{LMC}} = 18.55 \pm 0.10,$$

for the LMC. The error bar has been (subjectively) increased to account for systematic errors that may be rather large for this technique (note that this is totally irrelevant in the following discussion).

d) *SN1987A*

The "light echo" of SN1987A has been used by several different authors to derive an independent estimate of the LMC distance modulus. A rather small value of  $\mu_{\text{LMC}} < 18.37 \pm 0.04$  (possibly increased to 18.44 for an elliptical shape of the supernova expansion ring) was obtained by Gould & Uza (1998). This determination has been criticized by Panagia, Gilmozzi & Kirshner (1998), since Gould & Uza used lines of different excitation when comparing absolute and angular ring size. If lines of comparable excitation are used, a larger distance modulus of  $\mu_{\text{LMC}} = 18.58 \pm 0.05$  is derived (this value includes a small 0.03 mag correction which takes into account the position of SN1987a within the LMC). Panagia et al. (1998) distance modulus is compatible with the upper limit of  $\mu_{\text{LMC}} < 18.67$  obtained by Lundqvist & Sonneborn (1998).

The light echo of SN1987A is a very important method, because it is the only one which is completely independent of reddening. The agreement between the distance modulus derived from this method and the finally adopted one is then a strong and crucial support to the Cepheid reddening scale used throughout the present paper.

e) *Eclipsing binaries*

This is a very promising technique which uses the eclipsing binaries detected in a number of systems (LMC, GCs, etc) to derive their distances (Paczyński, 1996). In practice, the orbital parameters (period, inclination and eccentricity), the luminosity-ratios, the size of the orbit, and the linear radii of the two components are derived from the light and radial velocity curves, and then combined with the surface brightness of each component (inferred from the observed colors) to derive the distance. Since detached eclipsing double line spectroscopic binaries have been discovered near the MS turn-off of a number of GCs (Kaluzny et al. 1996, 1997), a direct measure of the cluster distances via this technique should soon be feasible. The major shortcoming of this method is how to properly derive the surface brightness of the two components from the observed quantities (colors, line

ratios etc.). So far this technique has been applied to one eclipsing binary in the LMC (HV2274, Guinan et al. 1998). The derived distance modulus is  $\mu_{\text{LMC}} = 18.30 \pm 0.07$  for an adopted reddening value of  $E(B-V) = 0.12$  mag (as derived from the spectral distribution of the star). This reddening is only slightly larger than derived from Cepheids in the same direction of HV2274 ( $0.106 \pm 0.011$  mag). Udalski et al. (1998b) have reanalyzed HV2274. They derive  $\mu_{\text{LMC}} = 18.22 \pm 0.13$  assuming a reddening of 0.146 mag. Once again, this underlines the large sensitivity to reddening of distance determinations to the LMC.

These distance moduli, if confirmed once the other 10 binaries in Guinan et al. sample will have been analyzed, favour the "short" distance scale.

f) *The Red Clump*

The red clump stars are the metal-rich counterpart of the HB stars. Red clump stars have been detected in the Galactic Bulge by the OGLE microlensing experiment (Udalski et al. 1993, Kiraga, Paczyński & Stanek, 1997). A well defined red clump of solar-neighborhood stars is present in the CMD obtained from Hipparcos data at an absolute magnitude of  $M_V \sim 0.8$  mag (Jimenez, Flynn & Kotoneva, 1998). Since red clump stars are very numerous (the red clump is the dominant post-main-sequence evolutionary phase for most stars), and the observed dispersion in the mean clump magnitude is quite small, the red clump can be used as a "standard candle" for distance estimates. The first to use this technique for the LMC were Udalski et al. (1998a), who found a very short distance modulus of  $\mu_{\text{LMC}} = 18.08 \pm 0.15$ .

The applicability of the red clump method is based on two assumptions: first it requires that the absolute magnitude of the red clump does not depend on age and chemical composition and second, that the stellar populations in the various systems do not significantly differ (in age and metallicity) from the solar neighborhood red clump population. However, model calculations and observations of open clusters show that quite

large corrections are actually required (Cole, 1998; Girardi et al. 1998). Furthermore, reddening is important in this method too. Udalski himself (Udalski 1999) reconsidered this issue, and obtained  $\mu_{\text{LMC}} = 18.23 \pm 0.05$  using stars around four LMC clusters having low reddening (reddenings used for these clusters are from the maps by Schlegel et al. 1998, but in these directions the maps agree well with the values given by Cepheids). On the other hand, the age and chemical composition corrections used by Udalski are not universally accepted. Twarog, Anthony-Twarog & Bricker (1999) using metal-poor galactic open clusters with distances determined via main sequence fitting obtain a much larger distance modulus for the LMC ( $\mu_{\text{LMC}} = 18.42 \pm 0.16$ ). Romaniello et al. (1999) used multi-band observations of the region around SN1987A, and carefully discussed reddenings toward individual stars (reddening is rather large towards this direction of the LMC). They found an even larger value of  $\mu_{\text{LMC}} = 18.59 \pm 0.04 \pm 0.08$ . Finally, Piatti et al. (1999) suggested that the RGB clump in the LMC has a vertical structure; if confirmed, this would further complicate the data interpretation.

Given the large uncertainties still present in this method, we would give it no weight in our discussion.

g) *Miras*

The period-luminosity relation for Miras based on Hipparcos parallaxes for a sample of these variables, gives a distance modulus for the LMC of:  $\mu_{\text{LMC}} = 18.54 \pm 0.18$  (Van Leeuwen et al. 1997), in good agreement with the long distance scale.

#### 4. DISTANCES AND AGES OF GLOBULAR CLUSTERS USING HIPPARCOS SUBDWARFS

#### 4.1. Previous results

The subdwarf fitting technique is a very powerful method to derive distances to GCs (Sandage 1970). However, until the release of the Hipparcos catalogue this procedure was heavily hampered by the lack of local metal-poor dwarfs with accurate parallaxes (VandenBerg et al. 1996). Hipparcos has definitely enlarged the number and accuracy of the subdwarfs in the solar neighborhood, which can be used in the subdwarf fitting. Thanks to Hipparcos, parallaxes are no longer the major contribution to the total error of the subdwarf fitting distances to GCs. In fact, besides parallaxes, a number of different ingredients and assumptions enter into this technique, which all contribute to the final result (i.e. the derived distance moduli), and to its accuracy. They are: 1) magnitudes, colors, metallicities and reddenings of the calibrating subdwarfs; 2) photometry, metallicity and reddening of the cluster stars; 3) correction of the parallaxes for intervening observational biases; 4) corrections for the contamination by undetected binaries in the subdwarf sample and/or in the GC Main Sequences; and 5) evolutionary status of the subdwarfs used in the fitting.

Three different groups had access to the Hipparcos database for the field subdwarfs, before the whole catalogue was released to the general public: Reid (1997; R97), Pont et al. 1998 (PMTV), and our team (Gratton et al. 1997a; Paper I). After the publication of the Hipparcos catalogue, new analyses appeared (Reid 1998: R98; Chaboyer et al. 1998: C98; Grundahl et al. 1998). A *compendium* of the relevant parameters and of the main results achieved by these studies is given in Table 1. All the distance moduli are apparent. If only true moduli were given in the original studies, apparent ones were obtained using the quoted reddening (column 4 of Table 1) and a value of 3.1 for the ratio of total-to-selective extinction. Also given in Table 1 are the adopted metallicities, coming from the two major abundance scales presently available for GCs, namely Zinn & West (1984, as subsequently

updated and extended), and Carretta & Gratton (1997, CG). Other informations in Table 1 concern the number of calibrating subdwarfs used in the fitting, together with the spanned metallicity range, the apparent moduli corrected to account for the possible presence of contaminating binaries in the subdwarfs sample, and references for both cluster mean ridge lines and distance moduli.

Table 1 allows a quick comparison of the results obtained by different authors. PMTV (1 cluster, M92) essentially confirm the distance and age estimates based on the ground-based parallax observations; Paper I, R97, R98, C98, and Grundahl et al. (1998) consistently derive *longer* distances and, in turn, *younger* ages for the clusters in their samples. In the following we briefly discuss and compare these independent studies.

**(a) Reid 1997:** R97 primary calibrating subdwarfs include 15 stars with parallaxes measured by Hipparcos with  $\Delta\pi/\pi = 0.12$ , plus 3 stars from the Yale General Catalogue of Trigonometric Parallaxes (van Altena, Truen-liang Lee & Hoffleit 1995), at same precision limit. Photometric data and low dispersion spectroscopic metallicities for the calibrating subdwarfs were taken from Carney et al. (1994). Metal abundances for the 7 studied GCs were instead from Zinn & West (1984), and mainly based on low dispersion indexes. A direct comparison of the two metallicity scales is not possible, but they are certainly not the same, which is one of the major drawbacks of this first analysis. Appropriate Lutz-Kelker corrections were included. Only metal-poor and intermediate-metallicity clusters are studied, with reddening estimates from a compilation of different literature sources. No attempt was made to select clusters at low reddening contamination. All subdwarfs are used in the fitting, independently of their evolutionary status (4 of R97 primary calibrators are evolved objects with  $M_V < 5.0$ ), or their binary status (but binaries are excluded from the fittings).

**(b) Gratton et al. (1997a; Paper I)** derived subdwarf fitting distances for 9

clusters, six of which are in common with R97. There are a number of differences and, we think, improvements in Paper I with respect to R97 analysis:

- a larger sample of subdwarfs (34 stars, 22 of them with  $[\text{Fe}/\text{H}] < -0.9$ )
- a careful reduction of the photometric data for the field subdwarfs to a consistent scale
- the strict homogeneity in the metal abundances of field *and* cluster stars (see however Section 4.8). High resolution spectra were obtained for most of the subdwarfs in their sample, and accurate abundances of Fe, O and  $\alpha$ -elements were derived (Clementini et al. 1999, CGCS99), following a procedure totally consistent to that used by CG for giants in GCs. For the remaining objects, new metallicities on the same metallicity scale were obtained through the re-calibration of low resolution abundance indicators (see CGCS99)
- a careful revision of the cluster photometries in order to eliminate possible inconsistencies. Nevertheless, an unambiguous and reliable photometric zero-point still lacks for some clusters (e.g. M92, see below Section 4.6)
- only clusters with interstellar reddening not exceeding 0.05 mag were analysed. Furthermore, in order to reduce reddening uncertainties still existing even for the best studied clusters, new reddening estimates were derived from the Strömgren and  $H_\beta$  photometry of B-F stars projected on the sky within 2 degrees from each cluster, and averaged to the previous literature estimates
- a careful procedure was devised in order to detect unknown binaries. Corrections were thus calculated as the product of the probability for a star to be a binary, and of the average correction for each binary, derived from the offset of the known binaries from the  $(B - V)_{Mv=6} - [\text{Fe}/\text{H}]$  relation

- finally, only *bona-fide* single stars on the unevolved portion of the main sequence ( $M_V < 5.5$ ) were used in the fittings

On average there is a reasonable agreement between Paper I distance moduli and R97, the mean difference being  $-0.08 \pm 0.04$  mag (six clusters, rms scatter of 0.09 mag): the distance scale of Paper I is then shorter than that of R97

(c) **Reid (1998)** partially revises R97 analysis and extends it to the metal-rich clusters, applying the MS fitting technique to 7 clusters, 3 of which were not included in R97. Besides an enlarged sample of calibrating subdwarfs and the improved treatment of the Lutz-Kelker corrections, the most relevant change in R98 analysis is the adoption of a metal abundance scale directly tied to high resolution spectroscopic analyses (i.e. CG) for the GCs, and of a very similar one for the subdwarf sample. Taking into account the existing differences in the calibrating sample, the adopted reddening and bias corrections, and within the quoted uncertainties, there is an overall agreement between R98 and Paper I (see Table 1 and R98 for further details). We note that R98 adoption, of a consistent metallicity scale for clusters and field subdwarfs, leads to halve the difference between R98 and Paper I distance moduli of NGC 6205, 6752 and 5904.

(d) **Pont et al. (1998)** had access to the whole Hipparcos catalogue just after the final data reduction. Their calibrating subdwarfs were extracted from the "merger" of two distinct lists. The first one (330 stars) was formed by subdwarf candidates selected from various sources before the Hipparcos parallaxes were known; the second one (216 stars) was selected *a posteriori* from the whole Hipparcos catalogue on the basis of parallaxes and colors. Among these more than 500 candidates, PMTV selected 17 stars with claimed metallicity  $[\text{Fe}/\text{H}] < -1.8$ , that they used to define a fiducial sequence (from the unevolved region below the turn-off point up to the subgiant phase) to match the mean locus of the GC M92. Their result was a distance modulus ( $14.68 \pm 0.08$ ) very similar to that obtained by

previous studies based on subdwarf parallaxes measured from the ground, and an age of 14 Gyrs. Differences in the subdwarfs calibrating samples are not the origin of this contrasting result which are mainly due to PMTV different, and sometimes arbitrary assumptions on (i) whether and how large bias corrections should be applied to the Hipparcos parallaxes (this conversely reflects differences on how the calibrating subdwarfs were originally selected), (ii) which corrections should be applied to account for undetected binaries contaminating the subdwarf sample, and (iii) whether only unevolved subdwarfs should be used or also subgiant stars should be included in the fittings (Gratton et al. 1997b, Gratton, Carretta & Clementini, 1999).

(d) **Chaboyer et al. (1998)** initially selected stars using an *a priori* sample drawn from the whole Hipparcos catalogue. They then restricted their analysis to the unevolved stars with spectroscopic abundances, and discarded all known or suspected binaries (but they prefered to apply no correction for undetected binaries). With this procedure they end up with a rather small sample of only 7 subdwarfs, all in a quite restricted metallicity range. For this reason they only give distances to three GCs (NGC6752, M5 and M13) having a metal abundance within the range covered by the observed subdwarfs. Rather than using homogenous abundance and reddening analyses for field stars and GCs, they prefer to discuss each star individually, taking what they consider to be the best guess for each star. While some inhomogeneity may indeed be introduced by this practice, they try to account for it with the adoption of error bars somewhat larger than those assumed by other authors. On the whole, their results agree very well with those of Paper I and of the present paper, although their distance modulus for M5 is slightly shorter than ours.

(e) **Grundahl et al. 1998:** much less details are available for the analysis of Grundahl et al. (1998), who derived a distance to M13 of  $(m - M)_V = 14.44 \pm 0.10$ , in good agreement with Paper I, this paper, and C98.

Concluding this discussion, we wish point out two major issues that have been poorly stressed insofar:

- all these distance estimates are in agreement with or even longer than the long distance scale ( $0.19 < M_V(HB) < 0.51$  at  $[\text{Fe}/\text{H}] = -1.5$  and with a slope of 0.18 for the metallicity-luminosity relation for HB stars). This is much brighter than given by the short distance scale ( $M_V(HB) \sim 0.75$  at  $[\text{Fe}/\text{H}] = -1.5$ ). In turn, the ages implied for M92 range from 11.4 to 15.4 Gyr on the scale used throughout this paper, while the age of M92 given by the short distance scale is  $\sim 18.5$  Gyr
- **Hipparcos parallaxes are systematically smaller than those previously obtained from ground.** This, by itself, directly translates into a "stretching" of the GC distances, and, in turn, in a 2-3 Gyrs decrease of their ages (in Paper I we computed a mean magnitude difference of  $0.20 \pm 0.04$  mag, limiting our attention to stars with  $\Delta\pi/\pi < 0.12$ ). Large, corrections must be applied to transform these smaller parallaxes into distance moduli that are very similar to the older values obtained from larger parallaxes

#### 4.2. New results using the overall HIPPARCOS database

Since the whole Hipparcos catalogue is now a public resource, it is possible to exploit its entire database in order to improve the subdwarf fitting analysis. Two different routes may be followed: i) to use an *a priori* sample where stars are selected according to criteria not based on Hipparcos parallaxes (as in R97, R98 and Paper I), ii) to use an *a posteriori* sample extracted from the whole Hipparcos color magnitude diagram (as in C98, and, in part, in PMTV).

The main difference between these two approaches is the number and relevance of

the statistical biases associated to intervening selection effects. In fact, while in a *a priori* selected sample, selection criteria (and corresponding biases) are known as they are defined by the investigators themselves, any *a posteriori* selected Hipparcos sample is hampered by the poor knowledge of the selection criteria originally applied to form the Hipparcos catalogue itself, and by the increasing incompleteness of the catalogue towards faint magnitudes ( $V > 7$ ). In particular, the metallicity of an *a posteriori* selected sample of subdwarfs, as well as the rate and distribution of secondary components of the contaminating binaries, are rather poorly defined, thus rendering very uncertain the correction of the corresponding systematic effects.

In the following Sections, we discuss these two approaches in details. According to the procedure outlined in Paper I, preference is given to the *a priori* sample approach, while the *a posteriori* sample is used to show how uncertainties, or different assumption about reddening, metallicity scale and binary corrections, can affect the analysis, and to test the completeness achieved by the *a priori* selected sample.

#### 4.2.1. The *a priori* sample

Stars of the *a priori* sample were extracted from the catalogues of Gratton, Carretta & Castelli (1997, GCC), Carney et al. (1994), Axer, Fuhrmann & Gehren (1994), Ryan & Norris (1991) and Schuster & Nissen (1989). We selected all the stars with  $V < 12$  and a metallicity  $[\text{Fe}/\text{H}] < -0.9$  (after correcting the original values to GCC scale). This sample includes about 400 stars and constitutes almost a proper motion limited sample. About 60% of the sample (246 objects) has parallaxes measured by Hipparcos. Most of the missing stars are faint objects. In fact, all stars with  $V < 9$  and about 88% of stars with  $9 < V < 10$  in our original sample are contained in the Hipparcos catalogue. This fraction decreases to about 50% and less than 30% in the magnitude ranges  $10 < V < 11$  and  $11 < V < 12$ ,

respectively.

Thus, as far as the metal-poor dwarfs are concerned, the Hipparcos catalogue seems to be almost complete, or at least adequately representative, down to  $V < 10$ . The introduction of a selection criterion based on the parallax accuracy changes dramatically the situation, because the median errors of Hipparcos parallaxes increase with apparent magnitude (they are less than 1 mas for  $V \leq 7.5$ , around 1.3 mas  $V \sim 9$ , and  $> 2$  mas for  $V > 10.5$ ). If, following Paper I, we cut the sample to stars with  $\Delta\pi/\pi < 0.12$ <sup>7</sup>, we are left with only 56 objects, all brighter than  $V = 10.5$ . Stars fainter than this limit are of only limited use for the present purpose.

In their fitting of the M92 sequence PMTV used also a few subgiant stars with  $M_V < 3.6$ . Seven subgiants are present in our *a priori* sample. Since stars with  $M_V < 3.6$  must be brighter than  $V \leq 8.8$  in order to have parallaxes with  $\Delta\pi/\pi < 0.12$ , and since our sample seems quite complete for  $V < 9$  (see next subsection), we are confident that most of the metal-poor subgiant stars with good parallax are present in our sample. Unfortunately, a good parallax is not a sufficient condition to use these stars for distance determinations. In fact:

- HD17072 is probably a HB star (see Gratton 1998b, Carney, Lee & Habgood 1998); HD6755 is too evolved, and HD89499 is out of any possible fitting relation
- reddening estimates for HD132475, HD140283, HD189558 (all included in the PMTV sample) and HD211998 are quite large and uncertain

---

<sup>7</sup>While this cut is arbitrary, we found it to be a good compromise to achieve a large enough sample of mainly metal-poor objects, with still small individual errors and Lutz-Kelker corrections. The extension to objects with  $\Delta\pi/\pi < 0.2$  does not provide additional useful informations

- HD211998 is a very close visual binary

More interesting for the purpose of deriving GC absolute ages are the unevolved stars close to the Zero Age MS ( $5 < M_V < 8$ ). We have 30 such objects with  $\Delta\pi/\pi < 0.12$  in our *a priori* sample. None of them has metal abundance  $[\text{Fe}/\text{H}] < -2$ , and 9 (2 of which are binaries) have  $[\text{Fe}/\text{H}] < -1.5$ . In Paper I we considered 33 stars in this absolute magnitude range; however, 12 of them had metallicity  $[\text{Fe}/\text{H}] > -0.9$  and are then excluded from the present discussion. Seven of these stars (2 binaries) have  $[\text{Fe}/\text{H}] < -1.5$ . We have then 9 additional metal-poor stars with good parallaxes; 2 of them are *bona fide* single stars with  $[\text{Fe}/\text{H}] < -1.5$ .

Finally, we note that all 9 stars with  $[\text{Fe}/\text{H}] < -1.5$  have  $(B - V)_{Mv=6} < 0.65$ . On the other side, approximately half of the 21 stars with  $-1.5 < [\text{Fe}/\text{H}] < -0.9$  have  $(B - V)_{Mv=6} < 0.65$  (11 stars, 2 binaries) and the remaining half (10 stars, 4 of which are binaries) have  $(B - V)_{Mv=6} > 0.65$ . This suggests that, in this range of magnitude, selecting stars with  $(B - V)_{Mv=6} < 0.65$  corresponds to obtaining a complete sample of objects with  $[\text{Fe}/\text{H}] < -1.5$ . However, samples selected using these criteria should be considerably contaminated by more metal-rich stars.

Table 2 summarizes the relevant data for the 56 stars with  $\Delta\pi/\pi < 0.12$  in the *a priori* sample.

$V$  magnitudes are the average of Carney et al. (1994), Ryan & Norris (1991) and Schuster & Nissen (1989) values, together with values from both Hipparcos and Tycho catalogues. Reddening values are obtained by averaging estimates from the 3 above-mentioned sources, or by adopting a cosecant law (Bond 1980), when such estimates are lacking. Absolute magnitudes include Lutz-Kelker corrections (see Sections 4.3 and 4.4.1).  $B - V$  colors are the weighted average of Carney et al., Ryan & Norris (with an arbitrarily adopted error of 0.01 mag) and Hipparcos/Tycho values (with the errors

quoted in the catalogue). Colors in Table 2 are de-reddened and errors include an adopted uncertainty due to reddening of 0.015 mag, for all stars. Whenever available, metallicities were from high resolution spectroscopic analyses (e.g. GCC, Axer et al., 1994, etc.), and tied to GCC/CG homogeneous metallicity scale. A weighted mean of the metallicities from Carney et al. (cross correlation dips), Ryan & Norris (low dispersion spectroscopy) and Schuster & Nissen (Strömgren photometry), corrected to GCC scale, was adopted for the stars lacking high resolution spectroscopy. An uncertainty of 0.15 dex, was assumed in this case. Finally, information on binarity is given, with the same meaning of Table 1 of Paper I.

#### 4.2.2. *The a posteriori sample*

As an alternative approach, a sample of metal-poor stars was extracted from the total color-magnitude diagram of the Hipparcos catalogue. This *a posteriori* approach is similar to the procedure used by PMTV to form their second sub-sample of 216 stars, and to the procedure followed by C98. From the available database we first extracted all stars with positive parallax and  $\Delta\pi/\pi < 0.12$  in the magnitude range  $5.0 < M_V < 8.0$  mag (4342 stars; this magnitude range should include mainly unevolved MS stars). Metal-poor candidates were then identified by inferring the metallicity from the  $B - V$  color given in the catalogue.

By shifting the location of an unevolved star in the color-magnitude diagram parallel to the main sequence (see Section 3 of Paper I), it is possible to derive its  $B - V$  at an absolute magnitude of  $M_V = 6$ ,  $(B - V)_{M_V=6}$ . In the range of interest, this color is predicted by theoretical models to be an approximately quadratic function of metallicity, decreasing the metal abundance giving bluer MSs (see equation 4 in Paper I). This relation was used to extract the *metal-poor* subdwarf candidates from the whole *a posteriori* selected unevolved stars with  $\Delta\pi/\pi < 0.12$ . We found that the number of metal-poor stars below the MS is very small: there are only 52 stars (1.2%) with  $(B - V)_{M_V=6} \leq 0.65$  (i.e.  $[\text{Fe}/\text{H}] < -1$ )

and  $\Delta\pi/\pi < 0.12$ . We caution, however, that metallicities deduced from colors may be overestimated (and, correspondingly, the number of metal-poor stars underestimated) since stars can be made redder by the interstellar reddening or by the presence of binary companions. These effects are balanced only in part by the Lutz-Kelker bias (stars that for erroneous measurements are below their true position have higher probability of being selected thus making the derived sequence bluer).

The problem is further complicated since the metallicity distribution of the stars in the solar neighbourhood is strongly skewed toward solar values. As a consequence, symmetrically distributed random color errors shift more stars in the lower metallicity bin than in the high metallicity one. An additional complication is the non-gaussian distribution of errors in the color data sets; e.g. in the Tycho catalogue there is a small but not negligible number of stars ( $\sim 1\%$ ) with color errors that may be as large as several tenths of a magnitude. Given these large errors, solar metallicity stars may be sometime erroneously interpreted as extremely metal-poor objects. The fraction of stars with large random color errors [ $\Delta(B - V) > 0.05$  mag] in the Tycho catalogue is comparable to (actually larger than) the fraction of metal-poor stars (with  $[\text{Fe}/\text{H}] < -1$ ) in the Hipparcos catalogue. A large contamination of spurious objects is then expected for the bluest bins in  $(B - V)_{Mv=6}$ .

This *metallicity bias* has a large impact on the *a posteriori* sample, where metallicities are derived from colors, while does not affect stars in the *a priori* sample, whose metallicities are known independently of colors. This is an important difference and a reason to definitely prefer the *a priori* approach.

### 4.3. Detecting, understanding and correcting for biases

*A priori* and *a posteriori* samples are both affected by a number of biases that must be taken into account in order to derive statistically corrected distances (and ages) of GCs. They are briefly discussed below.

#### 1. Lutz-Kelker effect and Malmquist bias

Average luminosities for sample of stars selected according to their absolute magnitudes (i.e. parallaxes) are affected by the Lutz-Kelker (1973) effect. This bias arises from the combination of measurement errors in the parallaxes (which are symmetric) and the strongly skewed distribution of true parallaxes. The net effect is a trend to include, and with more weight, stars with parallaxes measured too high, rather than stars with parallaxes measured too low. If not corrected, this bias leads to underestimate the average distance of the sample. Furthermore, due to classical Malmquist bias, the sample will likely contain more stars whose magnitudes are erroneously measured too bright vs stars with magnitude measured too faint. The corresponding average magnitude will thus be systematically overestimated. Given the small range in  $M_V$  of the subdwarf sample, this effect is small in G97, C98, and the present paper, while should be accounted for in R97, 98 and PMTV who used also turn-off stars in their fittings.

The Lutz-Kelker bias affects both the *a priori* and the *a posteriori* samples.

#### 2. Interstellar reddening

The interstellar reddening absorbs light coming from a star, thus weakening its magnitude, and reddens its color, thus simulating a higher metallicity for the stars in the *a posteriori* sample<sup>8</sup>. Although we have restricted the samples to stars with very accurate parallaxes

---

<sup>8</sup>The effect is much smaller and of opposite sign for stars in the *a priori* sample, since temperatures used in abundance analysis would be underestimated because of reddening,

(i.e. generally nearby objects), significant reddening corrections may still be required in a few cases.

### 3. Contamination by binaries

A binary MS companion may brighten and redden the intrinsic  $(B - V)_{Mv=6}$  color of the star under consideration, the amount of reddening actually depending on the magnitude difference between the two components. If the unresolved binary system is formed by stars with similar masses (and then luminosity), the primary component brightness can be spuriously enhanced of up to 0.75 mag (corresponding to the case of strictly equal masses). In turn, such star will more likely be included in the sample due to Malmquist bias.

### 4. Metallicity bias

As described in Section 4.2 this bias arises from the metallicity distribution of the stars in the Hipparcos catalogue. This bias requires large corrections; however it only affects the *a posteriori* selected sample<sup>9</sup>.

In order to properly take into account and correct for all the above biases, one should in principle have an exact knowledge of (i) spatial and metallicity distributions of the calibrating stars, (ii) distribution of measuring errors, (iii) distribution in mass of the secondary components in binary systems etc. Since all these quantities are generally poorly

---

and, in turn abundances would be underestimated

<sup>9</sup>It should be mentioned that a small metallicity bias affects also the *a priori* sample. In fact, since only stars with measured  $[\text{Fe}/\text{H}] < -0.9$  are selected, close to this limit only stars with negative errors are included, and average metallicities are thus underestimated. However, the net effect is small because errors in metallicity are small ( $\leq 0.15$  dex). The validity of the adopted interpolating relation between metallicity and MS color was checked using stars much more metal-rich than this limit

known, the safest approach is to restrict the analysis to (a) only stars with very accurate parallaxes; (b) very low reddenings; (c) discard binaries; and (d) use the *a priori* sample approach since this sample is not affected by the *metallicity bias*.

The *a posteriori* sample may however be used to check the completeness achieved by the *a priori* sample. There are 54 candidate metal-poor (i.e.  $(B - V)_{M_V=6} < 0.65$ , corresponding to  $[\text{Fe}/\text{H}] < -1.1$  using eq. 4 in Paper I), unevolved ( $5 < M_V < 8$ ) stars with good parallaxes (i.e.  $\Delta\pi/\pi < 0.12$ ), in the *a posteriori* sample. 22 of these stars have large errors associated with their  $(B - V)$  colors ( $\Delta(B - V) > 0.05$  mag) and should be discarded. Most of these objects are known visual binaries not separated by the Hipparcos beam; colors for these stars cannot be trusted. If we eliminate all stars with such large color errors, we are left with 32 stars. Reliable metal abundances exist in the literature for 26 of them (but only 11 are from high dispersion spectroscopy). According to these determinations 6 of these stars have metallicity  $[\text{Fe}/\text{H}] > -0.9$ , thus falling outside the range defining the metal-poor stars. It is also interesting to note that while all the 9 objects having  $[\text{Fe}/\text{H}] < -1.5$  are included in the *a priori* sample; *viceversa*, 9 stars of the *a priori* sample with metallicity  $[\text{Fe}/\text{H}] < -1.1$  (from high resolution spectroscopy) are *not* included in the *a posteriori* sample, since their too red measured colors lead to derive metal abundances  $[\text{Fe}/\text{H}] > -1.1$ .

In summary, the *a posteriori* sample contains only 6 new good candidate metal-poor stars (i.e. with  $[\text{Fe}/\text{H}] < -1.1$ ); 3 of them have  $(B - V)_{M_V=6} < 0.63$  (corresponding to  $[\text{Fe}/\text{H}] \leq -1.25$ ) and only one star has a color appropriate for  $[\text{Fe}/\text{H}] < -1.5$ . Noteworthy, even in this sample there is no star with  $[\text{Fe}/\text{H}] < -2$ .

According to these numbers, in the *a priori* sample there are 20 stars with  $(B - V)_{M_V=6} < 0.65$  and  $[\text{Fe}/\text{H}] < -1.1$  over a total number of good candidates found in the *a posteriori* sample ranging from 20 to 26 (adding the 6 new good candidates). We can

then estimate that the *a priori* sample is from 77 to 100% complete, the exact percentage depending on the fraction of the metal-poor candidates that actually are metal-poor stars. Taking into account the strong asymmetry in the metallicity distribution of the stars in the solar neighborhood, we estimate that the *a priori* sample is  $\sim 90\%$  complete.

We conclude that the *a priori* approach yields a quite complete sample. Furthermore, the cleaner definition of the intervening biases and corresponding corrections, makes it more reliable than the *a posteriori* based analysis, where the noticeable contamination of the sample forces the application of large and uncertain corrections. In the following Section, we describe the use of the extended list of unevolved stars with accurate parallaxes and reliable abundance determinations in the *a priori* sample, as fiducial calibrators to derive new distances for the 9 clusters studied in Paper I. The comparison with specific points of other studies will be also discussed, where needed.

#### 4.4. Analysis of the *a priori* sample

Basic data for the new calibrating subdwarfs are described in Section 4.1 and shown in Table 2. Since stars used in the analysis come from a larger original population (all stars with  $[\text{Fe}/\text{H}] < -1$ ,  $V < 12$ , and with parallax measured by Hipparcos with accuracy  $\Delta\pi/\pi < 0.12$ ), and since a weight proportional to  $(\pi/\Delta\pi)^2$  is associated to individual values, it is necessary to apply Lutz-Kelker corrections. These must be derived from the properties of the original sample.

##### 4.4.1. Lutz-Kelker correction

Following the procedure by Hanson (1979), we used the proper motions in the Hipparcos catalogue to derive Lutz-Kelker corrections of the parallaxes (i.e. absolute

magnitudes) of our calibrators. The proper motion distribution of the stars in the *a priori* sample is shown in Figure 2. This follows very well a power law described by the relation  $\mu^{-n}$ , where  $n$  is related to the corresponding parallax distribution ( $\sim \pi^{-n}$ ). For values of  $\mu > 0.25$  arcsec/yr (see Figure 2),  $n = 3.62 \pm 0.13$ . Since about the 80% of the original sample (i.e. the 246 stars from which the *a priori* sample was drawn) is included in this limit of  $\mu$  and since stars with  $\Delta\pi/\pi < 0.12$  form only  $\sim 20\%$  of this original sample, it seems appropriate to assume that parallaxes around this threshold are distributed as  $\pi^{-3.62 \pm 0.13}$ . This exponent of the parallax distribution is very close to the value ( $n = 4$ ) expected for a uniform distribution. This implies that the adopted magnitude cut ( $V = 12$ ) is not too much severe (for a comparison, R97 finds  $n = 3.4$ ). According to this value of  $n$ , the absolute magnitudes of our calibrators were corrected using the relation:

$$\Delta M_{LK} = -8.94 (\Delta\pi/\pi)^2 - 63.92 (\Delta\pi/\pi)^4 \quad (1)$$

We note anyway that given the severe limit in the parallax error, the Lutz-Kelker corrections for our sample are however rather small, the maximum value being  $\Delta M_{LK} = 0.14$  mag (the average being 0.02 mag).

#### 4.4.2. *Binary contamination*

Among the 56 stars in the *a priori* sample having good parallax ( $\Delta\pi/\pi < 0.12$ ), 19 (i.e. 34%) are known or suspected binaries. This binary fraction is smaller than in Paper I (47%: 16 out of 34 stars), but we believe this is simply due to the lack of accurate observations for most of the additional stars in this more extended sample. Therefore, a larger fraction of unknown binaries is expected to contaminate the candidate *bona fide* single stars of the present sample.

We have compared the residual distribution with respect to the  $(B - V)_{Mv=6} - [\text{Fe}/\text{H}]$

relationship (eq. 4 of Paper I) of both known binaries and *bona fide* single stars (in the range  $5 < M_V < 8$ ) in the extended sample, in order to estimate the systematic correction required to properly take into account the binary contamination. According to the procedure devised in Paper I (see Section 5.1 of that paper), we write this correction as the product of the probability of a star to be a binary and of the average correction for each binary. Using the present sample, we derived a probability of  $0.15^{+0.5}_{-0.15}$  for *bona fide* single stars to actually be binaries (as expected, this figure is larger than found in Paper I), and an average correction (derived from the average offset of the known binaries with respect to the  $(B - V)_{M_V=6} - [\text{Fe}/\text{H}]$  relation) of  $0.13^{+0.10}_{-0.13}$  mag. Therefore, the appropriate binary correction to apply to *bona fide* single stars in the present *a priori* sample is  $0.02^{+0.06}_{-0.02}$  mag.

Although a larger number of binaries are expected in the field than among cluster stars, where wide, primordial binaries are likely to be destroyed by interactions with other cluster stars, some contamination by undetected binaries may still affect the MS loci of the clusters in our sample. Moreover, blending of stars in the crowded field of GCs may mimic the physical binarity.

A search for binaries in the outer regions of some GCs has led to a binary occurrence of  $\leq 20\%$  (Pryor et al. 1989; Kaluzny et al. 1998; Rubenstein & Bailyn 1997; Ferraro et al. 1997), but larger values are found by (Fischer et al. 1994; Cote et al. 1994) based on radial velocity surveys with Fabry-Perot spectrographs.

The use of modal instead of mean values to identify the MS mean loci of GCs (e.g. Sandquist et al. 1996) may help reducing this effect. However, we used a Monte Carlo simulation and estimate that a residual "reddening" of about  $\sim 0.005$  mag (with an uncertainty of about 50%) might be present in the c-m diagrams used in our analysis. In turn, distance moduli could be corrected by  $\sim 0.03 \pm 0.02$  mag, in the sense to increase distances. However, given its large uncertainty we did not apply this correction.

#### 4.4.3. The $(B - V)_{Mv=6}$ –[Fe/H] relation

The goodness of the  $(B - V)_{Mv=6}$ –[Fe/H] derived in Paper I (Equation 4) was checked using the enlarged sample of subdwarfs of the present *a priori* sample. Only stars with  $5 < M_V < 8$  mag were used to perform this test (30 out of 56 objects in the sample). Results are illustrated in Figure 3, where filled symbols indicate *bona fide* single stars and open symbols are used for known or suspected binaries. Plotted over the data are the theoretical relations of Straniero & Chieffi (1991)<sup>10</sup>.

On average, the *bona fide* single stars are  $0.005 \pm 0.007$  mag ( $\sigma = 0.033$  mag) redder than the adopted relation with no clear trend with metallicity. This small (not very significant) difference could be due to undetected binaries which contaminate the sample.

We explicitly note that the observed  $(B - V)_{Mv=6}$ –[Fe/H] relation must be extrapolated, when considering the most metal-poor clusters (e.g. M92), since there are no unevolved stars with good parallax and  $[\text{Fe}/\text{H}] < -2$ , in the *a priori* sample. This is not an intrinsic limit of our sample though, since the comparison with the *a posteriori* sample assures that the lack of subdwarfs with very good parallaxes and metallicities lower than  $\sim -2$  dex is indeed an intrinsic limitation of the Hipparcos catalogue<sup>11</sup>.

---

<sup>10</sup>We used [m/H] rather than [Fe/H], in order to include the 0.3 dex enhancement due to the  $\alpha$ -elements, since this was not taken explicitly into account in these models

<sup>11</sup>The apparent presence of more metal-poor stars in PMTV sample is simply due to their adoption of a lower metal abundance scale. All of the most metal-poor stars in PMTV sample are also present in our *a priori* sample, but we attribute them a higher metallicity

#### 4.5. Globular Cluster distances and ages using MS fitting results

The new dataset of field subdwarfs selected *a priori* was used to re-derive distances and ages for the 9 GCs already studied in Paper I. The same data for the clusters (photometry, reddening, etc.), and the same general criteria and procedures defined in Paper I were adopted in the present analysis, with two main differences: i) we used all the stars with  $5 < M_V < 8$  mag; CD-80<sup>0</sup>328 and HD121004 were discarded though, since they yield very discrepant results (in opposite directions; we suspect colors or metal abundances for these two stars to be wrong), and ii) we considered only stars whose metal abundances were within 0.5 dex from that of the analyzed cluster. Colors for the subdwarfs were corrected following eq. 4 of Paper I, to account for differences in metallicity between clusters and calibrating subdwarfs.

Figure 4 shows the best fittings of the cluster mean loci to the fiducial sequences defined by the local calibrators. Only *bona fide* single stars with  $5 < M_V < 8$  were used in the fits. Relevant results obtained from the fittings are summarized in Table 3.

The absolute ages shown in this table were derived from Straniero, Chieffi & Limongi (1997) calibration of the turn-off luminosities. This set of model isochrones uses a value of  $M_{V_\odot} = 4.82$  mag, as recommended by Hayes (1985), and provides ages which fall in the middle of those obtained using other isochrone sets. Indeed, almost any of the most recent models result into very similar ages, once, as discussed in Paper I, the same luminosity-to-magnitude transformation is used. The new determinations compare very well with the results of Paper I. On average, the new distance moduli are 0.04 mag shorter, and the corresponding ages 0.5 Gyr larger, than in Paper I. In turn, there is again overall agreement between the present paper, R98 and C98. In this respect, thanks to R98 adoption of GCC metallicity scale, the difference in the distance moduli is decreased from  $\langle \Delta(m - M)_V \rangle = -0.07 \pm 0.03$  mag, *r.m.s.* = 0.08 mag (6 clusters) of [Paper I – R97], to

$\langle \Delta(m - M)_V \rangle = -0.03 \pm 0.02$  mag, *r.m.s.* = 0.05 mag (5 clusters) of [the present paper – R98].

#### 4.6. The case of M92

The GC M92 deserves a deeper discussion since it is often considered the prototype of an old GC, and because its distance modulus, as derived by independent MS fitting analyses, spans a range of about 0.30 mag (Table 1). The distance modulus we derive here for M92, without binary correction [ $(m - M)_V = 14.74$  mag], is identical to the value obtained by PMTV, again without binary correction. However this coincidence is totally fortuitous since (i) a different (lower) metallicity, (ii) a different (higher) reddening, and (iii) a much larger binary correction is assumed by PMTV for the subdwarf calibrators used to fit the M92 MS. Indeed, a number of arguments makes the application of the subdwarf fitting technique to M92 difficult and, the corresponding estimated distance and age uncertain:

- a) the zero-point of M92 photometry is still uncertain. There is a 0.03 mag difference in the color of the M92 MS, between the photometries of Heasley & Christian (1986) and Stetson & Harris (1988), the latter being bluer (thus yielding a longer modulus and a younger age). While Stetson & Harris photometry seems very reliable, a small zero-point error of  $\pm 0.01$  mag may still be present in the colors (Stetson & Harris 1988). A similar error may be present in the reddening estimate. The effect of errors in metal abundances may also be as large as  $\pm 0.06$  dex, implying an uncertainty of  $\pm 0.03$  dex in the distance. Combining these facts, the internal uncertainty on the age for this single cluster amounts to about 2-2.5 Gyr, that is equal to the difference between the age we derive for M92 (14.8 Gyr) and the average value for all “old” clusters (12.3 Gyr).
- b) according to GCC and CG there are no subdwarfs with metallicity comparable

to M92 (i.e.  $[\text{Fe}/\text{H}] < -2$ ) and with reliable parallax in the Hipparcos catalogue. As mentioned above, this is an intrinsic limitation of the catalogue itself, and not of our sample. Indeed, R98 did not re-examine M92 and the other most metal-poor clusters, since Hipparcos measured only two very metal-poor subdwarf candidates. The claimed presence of stars with good Hipparcos parallaxes, unevolved and with  $[\text{Fe}/\text{H}] < -2$ , in PMTV and R97, is simply due to their adoption of Carney et al. (1994) metal abundances for the field subdwarfs. However, as found by CGCS, Carney et al. abundances are too low (by about 0.36 dex) for the most metal-poor stars. PMTV distance to M92 is similar to that derived in the present paper only because they use larger reddening for the field subdwarfs (from Arenou, Grenon & Gomez 1992), and this fortuitously offsets the difference due to metallicity.

In view of all the uncertainties still involved in the M92 analysis, the distance to this cluster has a large error bar, and care should be exerted before drawing any conclusion on the age of the *oldest* GCs from the analysis of just M92.

#### 4.7. The impact of the adopted metallicity scale on the Pop. II distance scale: some caveats

Due to the strong sensitivity of the subdwarf fitting method to metal abundance ( $0.4 < d(m - M)_V / d[\text{Fe}/\text{H}] < 1$ , the exact figure depending on  $[\text{Fe}/\text{H}]$ , see Paper I for a detailed discussion of this point) the use of a strictly homogenous metallicity scale for cluster and field stars may still be not enough to assure derivation of correct cluster distances and ages. Indeed, although we have used GCC/CG metallicity scale for all stars involved in the fittings, systematic errors may still be present because:

- 1) cluster abundances are usually derived from giants while field calibrators are dwarfs.

Our abundances are derived using model atmospheres extracted from Kurucz (1993) grid. However, these models may better reproduce real atmospheres of dwarfs than of giants (see Gratton, 1998a, and CGCS99). Thus, residual systematic differences could possibly exist between abundances derived for these two types of stars. We estimate that these differences may be as large as 0.1 dex.

2) As well known, metal-poor stars are expected to show a substantial enhancement of the abundances of  $\alpha$ -elements with respect to iron, ( $[\text{O}/\text{Fe}] \sim 0.45$ ,  $[\alpha/\text{Fe}] \sim 0.3$ ) due to the interplay of the evolutionary times of SN I and SN II progenitors. However, two recent papers revealed that there may be exceptions. Carney et al. (1997) derived  $[\text{Mg}/\text{Fe}] = -0.31$  for BD+80<sup>0</sup>245 ( $[\text{Fe}/\text{H}] = -1.86$ ), and King (1997) found  $[\text{Mg}/\text{Fe}] = -0.10$  for the common proper motion pair HD134439/134440 ( $[\text{Fe}/\text{H}] = -1.50$ ). Since distance determinations depend on the  $[\alpha/\text{Fe}]$  ratio (being  $0.3 < d(m - M_V)/d[\alpha/\text{Fe}] < 0.7$ , from Straniero & Chieffi 1991), the problem is to establish how large is the fraction of  $\alpha$ -underabundant, metal-poor stars.

The underabundance in field stars could possibly be correlated with kinematics, as suggested by the large apogalactic distance of HD134439/134440. We have used an independent sample of 39 stars with  $[\text{Fe}/\text{H}] < -1$  and  $[\text{Mg}/\text{Fe}]$  from Fuhrmann, Axer & Gehren (1995), and Zhao & Magain (1990), to test the actual existence of this kinematics induced underabundance. We found that only a small minority of the metal-poor stars have  $\alpha$ -underabundance, with no clear correlation with kinematics. The lack of  $\alpha$ -enhancement in a few halo stars should then have only very minor effects on distance derivations.

As a further check of the impact of anomalous  $\alpha$ -abundances in local subdwarfs, we have derived the distance modulus of the programme clusters eliminating the couple HD134439/HD134440 from the sample (BD+80<sup>0</sup>245 is not amongst our calibration subdwarfs). Changes are very small: on average, distance moduli are decreased by

$0.004 \pm 0.005$  mag, with no corrections larger than 0.02 mag. Such changes will be neglected hereinafter.

#### 4.8. Residual overall uncertainties in the subdwarf fitting distances and ages for Globular Clusters: future directions

The applicability of the subdwarf fitting technique rests on the assumption that the metal-poor field subdwarfs in the solar neighborhood are the local counterpart of the GC MS stars. Since a direct measure of the trigonometrical parallax of GC stars is not in the reach of present day instrumental capabilities [but will became feasible with the accomplishment of the GAIA (Lindgren & Perryman, 1996) mission] we must rely on this assumption. However, for a robust application of the method, field calibrators and cluster stars should be analyzed in a consistent way. Indeed, in our procedure we made a serious effort to reduce any systematics arising from possible differences in the treatment of field subdwarfs and GC MS stars. However, some residual uncertainties still exist. In table 4 we summarize the most relevant sources of uncertainties present in our application of the subdwarf fitting technique.

Since we only used subdwarfs (i) with a limited range in magnitude ( $5 < M_V < 8$ ), (ii) with very accurate parallaxes ( $\Delta\pi/\pi < 0.12$ ), and (iii) *a priori* selected, the statistical biases (Malmquist bias, Lutz-Kelker, metallicity bias) contribute only marginally ( $\sim 0.02$  mag) to the final error on the derived distance moduli. Contamination by binaries among field subdwarfs (when only *bona fide* single stars are used), or in the cluster MSs (when modal instead of mean is used to define the loci sequence loci), contribute an additional  $\sim 0.04$  mag.

Presently, the largest sources of uncertainty reside with (i) colors and photometric

calibrations, (ii) reddening, and (iii) metal abundances and metallicity scale, for both the subdwarf calibrators and the GC MS stars.

Due to the steepness of the MS, small errors in the photometry may cause large errors in the derived distance moduli. Furthermore, at present, the only color suited for the subdwarf fitting is the  $B - V$ , since reliable  $V - R$  and  $V - I$  colors are lacking for many of the field subdwarfs (see CGCS99) and near-infrared deep color magnitude diagrams are not available for most clusters.

To avoid systematic effects, field calibrators and cluster stars should be observed with the same instrumental configuration and in the same photometric system. However, given the large difference in luminosity between the two samples (about 10 mag) this is not feasible. Photomultipliers and filters for the Johnson-Cousins system are generally used for the field calibrators, while CCD's are used for the GCs. Magnitudes for the latter are then transformed to Johnson-Cousins by observation of Landolt's standards (Landolt 1983, 1992). Albeit considerable care is generally devoted to the calibrations of the GCs data, some uncertainty still exists, and results for individual clusters may well have rather large errors. We estimate a total photometric uncertainty of  $\sim 0.04$  mag (distance modulus) as the average over the 9 clusters considered here.

A consistent reddening scale should be used for cluster and dwarf stars. Up to now, a direct comparison of the excitation temperatures of field subdwarfs and GC MS stars has not been feasible (important progresses are expected from UVES at VLT2); however some constraints can be derived by comparing the reddenings adopted for GCs and template subdwarfs with a cosecant law. Reddenings for the GCs were taken from Zinn (1980), this procedure is common to R97,98, G97 and PMTV. Two different reddening scales are available, instead for the subdwarfs. In the present analysis we adopt reddenings from Carney et al. (1994), Schuster & Nissen (1989), and Ryan & Norris (1991). A star-by-star

comparison shows that they are on a uniform scale. PMTV reddening for the subdwarfs were instead taken from Arenou et al. 1992. When compared to cosecant-laws for reddening (Bond 1980), GCs and subdwarfs are on a uniform reddening scale if the height scale of the galactic dust disk is 100 pc in our reddening scale for the subdwarfs, and 40 pc if PMTV scale is adopted. While the former value is in the middle of current determinations of the galactic dust scale-height (50-150 pc: Lynga 1982, Pandey & Mahra 1987, Scheffler & Elsässer 1987, Spitzer 1978, Salomon et al. 1979, Burton 1992, Chen 1998), the latter is at the lower extreme of the admitted range.

On the whole, we think that the reddening scale of subdwarfs still carries an uncertainty of  $\pm 0.015$  mag; this translates into an uncertainty of  $\sim 0.07$  mag in the derived distance moduli.

Finally, differences in the adopted metallicities of subdwarfs and clusters stars may still be present even if a homogeneous metallicity scale was adopted, since abundance for clusters are derived from giants instead of MS stars. For this reason systematic differences (of  $\sim 0.1$  dex) may exist between the metallicity of the template subdwarfs and the GC stars. This translates into a corresponding uncertainty of  $\pm 0.08$  mag in the derived distance moduli.

As an example, Figure 5 displays the best fit of the 9 clusters analyzed in the present paper obtained assuming that CG metallicity for these clusters is underestimated by 0.1 dex. The fitting of the cluster subgiant branches seem to be slightly improved. However, a similar effect could also be produced by errors in the adopted reddenings for the few subgiants with good parallaxes used in the fits, or if the cluster reddening scale were systematically underestimated by  $\sim 0.01$  mag, well within the uncertainties of current reddening estimates for the clusters.

Adding up in quadrature the errors listed in Table 4 we obtain 0.12 mag as total error

budget associated with our subdwarf fitting distances to GCs. The analogous figure quoted in Table 2 of Renzini (1991) was 0.25 mag. At the time the Renzini’s paper was written, this large error was mainly accounted for by uncertainties in the parallax data. Thanks to Hipparcos this uncertainty has now been more than halved, and no longer resides with parallaxes, but with photometric calibrations, reddening and metallicity scales.

## 5. THE $M_V(HB)$ –[Fe/H] RELATION AND DISTANCE MODULUS OF THE LMC

### 5.1. Results from subdwarf fitting method

Using data listed in Table 3, we derive the following weighted best fitting relations between absolute magnitude of the HB and metallicity:

$$M_V(HB) = (0.13 \pm 0.09)([\text{Fe}/\text{H}] + 1.5) + (0.44 \pm 0.04) [\pm 0.12] \quad (2)$$

$$M_V(ZAHB) = (0.18 \pm 0.09)([\text{Fe}/\text{H}] + 1.5) + (0.53 \pm 0.04) [\pm 0.12] \quad (3)$$

$$M_V(RR) = (0.18 \pm 0.09)([\text{Fe}/\text{H}] + 1.5) + (0.47 \pm 0.04) [\pm 0.12] \quad (4)$$

Here 0.04 mag is the internal error, however as discussed in Section 4.8 a more realistic estimate of the error is 0.12 mag.

We recall that  $M_V(HB)$  is the average magnitude of the HB (see also Section 5.2.3 of Paper I). Due to evolution, this luminosity is somewhat brighter than the Zero Age HB luminosity  $M_V(ZAHB)$ , usually provided by theoretical models. Following Paper I we used Sandage (1993) relation to tie  $M_V(HB)$  to  $M_V(ZAHB)$ .  $M_V(HB)$  does not coincide either with the average magnitude of the RR Lyrae variables,  $M_V(RR)$ . We adopted Caloi et al. (1997) correction between  $M_V(ZAHB)$  and  $M_V(RR)$ .

In Paper I we estimated the age of the oldest GCs by considering only Oosterhoff II and Blue HB Clusters. If, however, we are rather interested in the epoch of formation of GCs, all the nine clusters of Table 3 should be considered (we incidentally note that deviations of individual clusters from the average value are of the same order of the expected accuracy of the internal errors of the MSF technique: more accurate relative ages can be obtained using other techniques). A simple average of the ages in Table 3 gives  $12.2 \pm 0.5$  Gyr ( $\sigma = 1.4$  Gyr r.m.s. of values for individual clusters). However, as discussed in Paper I, this error bar (as well as the simple mean value) is incorrect, because (i) systematic errors are much larger than random errors; and (ii) some of the error bars are not symmetric (for instance, uncertainties in the consideration of diffusion may only lead to reducing the ages of Table 3 which were derived neglecting diffusion). Following the approach of Paper I, we then estimated a more realistic error bar using a MonteCarlo technique. Table 5 lists the individual sources of errors considered in this simulation, as well as the type of distribution and the adopted parameters<sup>12</sup>. The resulting mean age for the nine GCs is:

$$\text{Age} = 11.5 \pm 2.6 \quad \text{Gyr} \quad (5)$$

(95% confidence range). While this value nearly coincides with that of Paper I, its meaning is different. In fact, in Paper I that was the age of the oldest GCs, here it represents the mean age of the galactic GCs. If the same cluster selection made in Paper I is made, we would derive an age of  $11.9 \pm 2.7$  Gyr.

---

<sup>12</sup>Among the other source of errors, we mention here that we assumed a flat distribution for  $[\alpha/\text{Fe}]$  between +0.2 and +0.5 dex, with a preferred value of +0.3 dex. We believe this is the best estimate from current determinations in the metallicity range which is relevant in the present context :  $-2 < [\text{Fe}/\text{H}] < -1$ . Adopting Chaboyer et al. (1998) age -  $[\alpha/\text{Fe}]$  dependence the corresponding error in ages ranges from  $-0.8$  to  $+0.3$  Gyr

Finally, using eq. (4) we derive the following estimates for the LMC distance modulus:

$$\mu_{\text{LMC}} = 18.64 \pm 0.04 [\pm 0.12]$$

for an adopted average dereddened magnitude of the RR Lyraes in the bar of the LMC  
 $\langle V_0 \rangle = 19.11 \pm 0.02$ .

## 5.2. Best estimate of the distance to the LMC and of the age of globular clusters

The LMC is widely considered a corner-stone of the astronomical distance scale. In Table 6 we have summarized different estimates of the distance modulus of the LMC obtained by a large number of independent techniques, some of which based on Hipparcos parallaxes (see Section 3). Our subdwarf fitting modulus for the LMC is slightly larger than those provided by the other techniques: however, **within their error bars almost all methods provide the same distance to the LMC. This result is new, and stems from the adoption of a consistent reddening scale in the various distance determinations. Once the same reddening scales are adopted for Cepheids and RR Lyrae, the short and long distance scale agree within their nominal error bar.** The only result which is clearly discrepant at present is that from the eclipsing binary HV2274 by Guinan et al.; if we accept its internal error as a realistic estimate of the true error bar, this result is more than  $3\sigma$  from the average of all other determinations. This might indicate that some problem still exists on the distance to the LMC; however, we (aribratirily) prefer to wait more data on eclipsing binaries in the LMC before assigning weight to this method.

If the distance to HV2274 is neglected, the (weighted average) distance modulus of the

LMC is:

$$\mu_{\text{LMC}} = 18.54 \pm 0.03 \pm 0.06,$$

where the first error bar is simply the  $1\sigma$  error bar due to scatter in the individual determinations, while the second one derives from an (arbitrarily) assumed uncertainty of  $\pm 0.02$  mag in the reddening scale.

The main implications of this result are:

1. The cosmic distance scale is  $2 \pm 2\%$  longer than previously assumed, and the value of the Hubble constant correspondingly smaller. The change with respect to the value usually assumed in extragalactic studies is small and may be reasonably neglected for most purposes.
2. The  $M_V(HB)$ –[Fe/H] relations implied by this distance scale are:

$$M_V(HB) = (0.13 \pm 0.09)([\text{Fe}/\text{H}] + 1.5) + (0.54 \pm 0.07) \quad (6)$$

$$M_V(ZAHB) = (0.18 \pm 0.09)([\text{Fe}/\text{H}] + 1.5) + (0.63 \pm 0.07) \quad (7)$$

$$M_V(RR) = (0.18 \pm 0.09)([\text{Fe}/\text{H}] + 1.5) + (0.57 \pm 0.07) \quad (8)$$

3. The ages of the GCs derived assuming this distance scale (which is  $1\sigma$  shorter than given by the subdwarf fitting method) are 1.4 Gyr older than found in Section 5, well within the quoted error bar. The average age of the GC would then be:

$$\text{Age} = 12.9 \pm 2.9 \quad \text{Gyr} \quad (9)$$

(95% confidence range).

## 6. THE EPOCH OF FORMATION OF GLOBULAR CLUSTERS AND THE COSMIC SFR

The Milky Way provides basic data to study the cosmic evolution of galaxies. However, up to a few years ago, the discrepancy existing between the age estimated for the galactic GCs and for the present and past expansion rate of the Universe hampered the use of this template. In particular, it was impossible to compare the epoch of formation of our own Galaxy with evidences from high redshift objects.

While large uncertainties still exist, the situation has now changed thanks to (i) the very recent results about the Universe de-acceleration parameters obtained by type Ia SNe studies (Schmidt et al. 1998; Perlmutter et al. 1998; Garnavich et al. 1998), and to (ii) the revised estimates of the age of the (old) galactic GCs now possible thanks to Hipparcos. In Figure 6, we have plotted the redshift of the formation of GCs against various possible values for the Hubble Constant. The three panels show the results obtained for three different values of  $\Omega_M$  (0.2, 0.3, and 0.4), within a flat Universe ( $\Omega_\Lambda = 1 - \Omega_M$ ). The solid line shows the favourite age of GCs according to the present paper (12.9 Gyr), and the dashed lines represent the limits of our 95% level of confidence. While the admitted area is still large, it is possible to locate at quite high confidence the epoch of formation of galactic GCs (that we identify with the first major episode of star formation in our Galaxy, corresponding to the bulk of the halo, the thick disk, and perhaps the bulge) at  $z > 1$  the preferred value being at  $z \sim 3$ .

This value for the epoch of formation of GCs compares well with evidences from high redshift galaxies, as given by analysis of the HDF, which locates the bulk of cosmic star formation at  $z \simeq 1$  (Madau et al. 1998). An older star formation (at  $1 < z < 4$ ) was obtained by Franceschini et al. (1998) for elliptical galaxies in the HDF (assuming  $q_0 = 0.15$ , roughly corresponding to  $\Omega_M = 0.3$ ). This comparison is perhaps more relevant here, since

our age estimate does not include the thin disk of the Milky Way, whose formation likely occurred later (see e.g. discussion in Gratton et al. 1996).

## 7. CONCLUSIONS

The literature of the last year has seen the flourishing of a number of new techniques to measure distances as well as a re-newed interest in the classical methods which have been revised in light of Hipparcos data (see Section 3).

A lively debate is taking place among authors who favour one method to the other and, in turn, one distance scale to the other. By significantly increasing the number of local subdwarfs with accurate parallaxes, Hipparcos has allowed to definitely improve the subdwarf MS fitting technique. Work still remains to be done, though. In fact, while waiting for the benefits of the next generation astrometric missions (GAIA, SIM see <http://sim.jpl.nasa.gov/sim/>), all the efforts should be devoted to cutting down the 0.12 mag residual uncertainty still affecting the MSF distances to GCs. New, deep, and precisely absolute-calibrated photometric data should be collected for GCs (M92 in particular), reddening determinations should be improved, and abundance analysis of cluster MS stars should be performed.

Based on our detailed analysis, the MS fitting method favours the *long* distance scale and provides a distance modulus for the LMC of :  $\mu_{\text{LMC}} = 18.64 \pm 0.04$  [ $\pm 0.12$ ], (based on  $\langle V_0 \rangle = 19.11 \pm 0.02$  for the RR Lyraes in the bar of the LMC), and an average age for the 9 analyzed clusters of Age =  $11.5 \pm 2.6$  Gyr.

Our subdwarf fitting modulus for the LMC is  $1\sigma$  larger than provided by other techniques. However, within their error bars all methods lead to the same distance to the LMC once the same reddening scale is adopted for Cepheid and RR Lyrae variables. Short

and long distance scales may be reconciled on an average distance modulus for the LMC bar of :

$$\mu_{\text{LMC}} = 18.54 \pm 0.03 \pm 0.06$$

The corresponding average age of the GCs would then be :

$$\text{Age} = 12.9 \pm 2.9 \quad \text{Gyr}$$

We wish to thank Dr. P.L. Bernacca and M. Lattanzi for their help to access the Hipparcos data, and Dr. C. Corsi and C. Sneden for their collaboration at an early stage of this research. We also thank M. Bolzonella, V. Castellani, S. Degl'Innocenti, M. Feast, M. Marconi, L. Moscardini and M. Zoccali for helpful and pleasant discussions. The financial support of Agenzia Spaziale Italiana (ASI) and of Ministero della Universita' e della Ricerca Scientifica e Tecnologica (MURST) is gratefully acknowledged.

This research has made use of the SIMBAD data base, operated at CDS, Strasbourg, France.

## REFERENCES

Alcock, C., et al., 1996, AJ, 111, 1146

Alcock, C., et al., 1997, AJ, 482, 89

Arenou, F., Grenon, M., & Gomez, A., 1992, A&A 258, 104

Axer, M., Fuhrmann, K., & Gehren, T., 1994, A&A, 291, 895

Baade, W., 1926, Astron. Nachr., 228, 359

Bolte, M., 1987a, ApJ 315, 469

Bolte, M., 1987b, ApJ 319, 760

Bolte, M., & Hogan C.J., 1995, Nature, 376, 399

Bond, H.E., 1980, ApJS, 44, 517

Bragaglia, A., Carretta, E., Gratton, R.G., & Clementini, G. 2000, in preparation

Buonanno, R., Corsi, C.E., & Fusi Pecci, F., 1989, A&A, 216, 80

Burton, W.B., 1992, in The Galactic Interstellar Medium, D. Pfenniger & P. Bartholdi eds. (Springer: Berlin) p. 1

Cacciari, C., Clementini, G., & Fernley, J., 1992, ApJ 396, 219

Caldwell, J.A.R. & Coulson, I.M., 1985, MNRAS, 212, 879

Caldwell, J.A.R. & Laney, C.D., 1991, IAU Symp. 148, The Magellanic Clouds, ed. R. Hayes and D. Milne (Dordrecht, Kluwer), p.549

Caloi, V., D'Antona, F., & Mazzitelli, I., 1997, A&A, 320, 823

Carney, B.W., Latham, D.W., Laird, J.B., & Aguilar, L.A., 1994, AJ, 107, 2240

Carney, B.W., Wright, J.S., Sneden, C., Laird, J. B., & Aguilar, L.A., 1997, AJ, 114, 363

Carney, B.W., Lee, J.W., & Habgood, M.J., 1998, AJ, 116, 424

Carretta, E., & Gratton, R.G., 1997, A&AS, 121, 95 (CG)

Cassisi, S., Castellani, V., Degl'Innocenti, S., & Weiss, A., 1997, A&AS, 129, 267

Castellani, V., 1999, in Globular Cluster, X Canary Winter School, eds. C. Martinez Rogers, F. Sanchez & P. Fournon, Cambridge Univ. Press, Cambridge, in press

Chaboyer, B., Demarque, P., Kernan, P.J., & Krauss, L.M., 1996, Science, 271, 957

Chaboyer, B., Demarque, P., Kernan, P.J., & Krauss, L.M., 1998, 494, 96 (C98)

Chen, B., 1998 private communication

Chieffi, A., Straniero, O., & Limongi, M., 1998, pre-print

Clementini, G., Carretta, E., Gratton, R.G., Merighi, R., Mould, J.R., & McCarthy, J.K., 1995, AJ, 110, 2319

Clementini, G., Gratton, R.G., Carretta, E., & Sneden, C., 1999, MNRAS, 302, 22 (CGCS99)

Clementini, G., Bragaglia, A., Di Fabrizio, L., Carretta, E. & Gratton, R.G., 1999, in IAU Coll. 176, on "The Impact of Large Scale Surveys on Pulsating Stars Research", Eds. L. Szabados & D. Kurtz, ASP Conf.Ser., in press, (astro-ph/9909332)

Clementini, G., Gratton, R.G., Bragaglia, A., Carretta, E., & Di Fabrizio, 2000, in preparation

Cole, A.A., 1998, ApJ, 500, L137

Cool, A.M., Piotto, G., & King, I.R., 1996, ApJ, 468, 655

Cote, P., Welch, D.L., Fischer, P., Da Costa, G.S., Tamblyn, P., Seitzer, P., & Irwin, M.J., 1994, ApJS, 90, 83

De Marchi, G., & Paresce, F., 1995, A&A, 304, 202

Di Benedetto, G.P., 1997, ApJ, 486, 60

Durrell, P.R., & Harris, W.E., 1993, AJ, 105, 1420

Elson, R.A.W., Gilmore, G.F., & Santiago, B.X., 1995, AJ 110, 682

Fahlman, G.G., Richer, H.B. & Vandenberg, D.A., 1985, ApJS, 58, 225

Fernley, J., 1994, A&A 284, L16

Fernley, J., Barnes, T.G., Skillen, I., Hawley, S.L., Hanley, C.J., Evans, D.W., Solano, E., & Garrido, R., 1998a, A&A 330, 515

Fernley, J., Carney, B.W., Skillen, I., Cacciari, C., Janes, K. 1998b, MNRAS, 293, L61

Feast, M. W., 1997, MNRAS 284, 761

Feast, M. W. & Catchpole, R. M., 1997, MNRAS, 286, L1

Ferraro, F., Carretta E., Fusi Pecci, F., & Zamboni, A., 1997, A&A, 327, 528

Fischer, P., Welch, D.L., Mateo, M., & Cote, P., 1994, AJ, 106, 1508

Franceschini, A., Silva, L., Fasano, G., Granato, G.L., Bressan, A., Arnouts, & S., Danese, L., 1998, ApJ, 506, 600

Fuhrmann, K., Axer, M., & Gehren, T., 1995, A&A, 301, 492

Fusi Pecci, F., et al., 1996, AJ, 112, 1461

Garnavich, P.M., et al., 1998, ApJ, 509, 74

Girardi, L., Groenewegen, M.A.T., Weiss, A., & Salaris, M., 1998, MNRAS, 301, 149

Gieren, W.P., Fouqué, P., & Gómez, M., 1998, ApJ, 496, 17

Gould, A., & Uza, O., 1998, ApJ, 494, 118

Gratton, R.G., 1998a, Mem.S.A.It., 69, 145

Gratton, R.G., 1998b, MNRAS, 296, 739

Gratton, R.G., 1998c, in proceedings of the workshop Evolving Evolution, Carloforte, June 1998, eds. T. Zanzu, V. Testa & M. Bellazzini, in press

Gratton, R.G., Carretta, E., & Castelli, F., 1997, A&A, 314, 191 (GCC)

Gratton, R.G., Fusi Pecci, F., Carretta, E., Clementini, G., Corsi, C.E., & Lattanzi, M.G., 1997a, ApJ, 491, 749 (Paper I)

Gratton, R.G., Fusi Pecci, F., Carretta, E., Clementini, G., Corsi, C.E., & Lattanzi, M.G., 1997b, in Hipparcos Venice'97 Symposium, Venezia, Ed. B. Battrick, ESA Publication Division, c/o ESTEC, Noordwijk, The Netherlands, ESA SP-402, 339

Gratton, R.G., Carretta, E., & Clementini, G., 1999, in Post-Hipparcos Cosmic Candles, Eds. F. Caputo, A. Heck, Kluwer Acad. Publ., Dordrecht, The Netherlands, p. 89

Grundahl, F., VandenBerg, D.A., & Andersen, M.I., 1998, ApJ, 500, 179

Guinan et al., 1998, ApJ, 509, L21

Hanson, R.B., 1979, MNRAS, 186, 675

Hayes, D.S., 1985, IAU Symp. 111, p. 225

Heasley, J.N., & Christian, C.A., 1986, AJ, 307, 738

Hesser, J.E., Harris, W.E., VandenBerg, D.A., Allwright, J.W. B., Shott, P., & Stetson, P., 1987, PASP, 99, 739

Hodder, P.J.C., Nemec, J.M., Richer, H.B., & Fahlman, G.G., 1992, AJ, 103, 460

Jimenez, R., Flynn, C., & Kotoneva, E., 1998, MNRAS, 299, 515

Jones, R.V., Carney, B.W., Storm, J., & Latham, B.W., 1992, ApJ, 386, 646

Kaluzny, J., Kubiak, M., Szymanski, M., Udalski, A., Krzeminski, & W., Mateo, M., 1996, A&AS, 120, 139

Kaluzny, J., Kubiak, M., Szymanski, M., Udalski, A., Krzeminski, & W., Mateo, M., & Stanek, K., 1997, A&AS, 122, 471

Kaluzny, J., Hilditch, R.W., Clement, C., & Rucinski, S.M., 1998, MNRAS, 296, 347

King, J.R., 1997, AJ, 113, 2302

Kiraga, M., Paczyński, B., & Stanek, K.Z., 1997, ApJ, 485, 611

Koen, C. & Laney, D., 1998, MNRAS, 301, 582

Kurucz, R.L., 1993, CD-ROM 13 and CD-ROM 18

Landolt, A.U., 1983, AJ, 88, 439

Landolt, A.U., 1992, AJ, 104, 340

Laney, C.D., & Stobie, R.S., 1993, MNRAS, 263, 921

Laney, C.D., & Stobie, R.S., 1994, MNRAS, 266, 441

Lasenby, A., 1998, in 19th Texas Symposium on Relativistic Astrophysics and Cosmology, p. 63

Layden, A.C., Hanson, R.B., Hawley, S.L., Klemola, A.R., & Hanley, C.J., 1996, AJ, 112, 2110

Lindgren, L., & Perryman, M.A.C., 1996, A&AS, 116, 579

Lilly, S.J., Le Fevre, O., Hammer, F., & Crampton, D., 1996, ApJ, 460, L1

Liu, T., & Janes, K.A., 1990a, ApJ, 354, 273

Liu, T., & Janes, K.A., 1990b, ApJ, 360, 561

Lundqvist, P., & Sonneborn, G., 1998, in SN 1987A: Ten Years After, eds. M. Phillips and N. Suntzeff, ASP Conf. Ser., in press

Lutz, T.E., & Kelker, D.H., 1973, PASP, 85, 573

Lynga, G., 1982, A&A, 109, 213

Madau, P., Ferguson, H.C., Dickinson, M.E., Giavalisco, M., Steidel, C.C., & Fruchter, A., 1996, MNRAS, 283, 1388

Madau, P., Pozzetti, L., & Dickinson, M.E., 1998, ApJ, 498, 106

Madore, B.F., & Freedman, W.L., 1995, ApJ 109, 1645

Madore, B.F., & Freedman, W.L., 1998, ApJ 492, 110

McClure, R.D., VandenBerg, D.A., Bell, R.A., Hesser, J.E., & Stetson P.B., 1987, AJ, 93, 1144

McNamara, D.H., 1997, PASP 109, 857

Mermilliod, J.C., Turon, C., Robichon, N., & Arenou, F., 1997, in HIPPARCOS Venice'97, ESA-SP 402, p. 643

Narayanan, V.K., & Gould, A., 1999, ApJ, 523, 328

Oestreicher, M.O., & Schmidt-Kaler, T., 1996, A&AS, 117, 303

Oestreicher, M.O., Gochermann, J., & Schmidt-Kaler, T., 1995, A&AS, 112, 495

Oudmaijer, R.D., Groenewegen, M.A.T., & Schrijver, H., 1998, MNRAS, 249, 410

Paczyński, B., 1996, in STScI Symposium on The Extragalactic Distance Scale, Baltimore, May 1996, astro-ph/9608094

Panagia, N., Gilmozzi, R., & Kirshner, R.P., 1998, in SN 1987A: Ten Years After, eds. M. Phillips and N. Suntzeff, ASP Conf. Ser., in press

Pandey, A.K., & Mahra, H.S., 1987, MNRAS, 226, 635

Pearlmutter et al., 1998, Nature 391, 51

Penny, A.J., & Dickens, R.J., 1986, MNRAS, 220, 845

Piatti, A.E., Geisler, D., Bica, E., Claria, J.J., Santos Jr, J.F.C., Sarajedini, A., & Dottori, H, 1999, AJ, in press (astro-ph/9909475)

Pinsonneault, M.H., Stauffer, J.R., Soderblom, D.R., King, J.R., & Hanson, R.B., 1998, ApJ, 504, 170

Pont, F., 1998, in Harmonizing Distance Scales in the post-Hipparcos Era, Haguenau, September 1998, eds. D.Egret & A.Heck, in press

Pont, F., Mayor, M., Turon, C., & Vandenberg, D.A., 1998, A&A, 329, 87 (PMTV)

Popowski, P. & Gould, A., 1998a, ApJ, 506, 259

Popowski, P. & Gould, A., 1998b, in Post Hipparcos Cosmic Candles, F.Caputo & A.Heck (Eds.), Kluwer Academic Publ., Dordrecht, p. 53

Pryor, C., McClure, R.D., Hesser, J.E., & Fletcher, J.M., 1989, in Dynamics of Dense Stellar Systems (Cambridge: Cambridge University Press) p. 175

Rees, Jr. R.F., 1996, in Formation of the Galactic Halo... Inside and Out, H. Morrison, & A. Sarajedini eds., ASP Conf. Ser. 92, p. 289

Reid, I.N., 1997, AJ, 114, 161 (R97)

Reid, I.N., 1998, AJ, 115, 204 (R98)

Renzini, A., 1991, in Observational Tests of Inflation, ed. T. Banday & T. Shanks (Dordrecht: Kluwer) 131

Renzini, A. et al., 1996 ApJ, 465, L23

Richer, H.B. et al., 1995, ApJ, 465, L23

Richer, H.B., & Fahlman, G.G., 1986, ApJ, 304, 273

Richer, H.B., Fahlman, G.G., & Vandenberg, D.A., 1988, ApJ, 329, 187

Romaniello, M., Salaris, M., Cassisi, S., & Panagia, N., 1999, ApJ, in press (astro-ph/9910082)

Rubenstein, E.P., & Bailyn, C.D., 1997, ApJ, 474, 701

Ryan, S.G., & Norris, J.E., 1991, AJ, 101, 1835

Salomon, P.M., Sanders, D.B., & Scoville, N.Z., 1979, in Large-Scale Characteristics of the Galaxy, IAU Symp. no. 84, Burton, W.B. ed., Reidel, Dordrecht, p. 35

Sandage, A.R., 1970, ApJ, 162, 841

Sandage, A.R., 1993, AJ, 106, 703

Sandquist, E. L., Bolte, M., Stetson, P. B., & Hesser, J. E. 1996, ApJ, 470, 910

Scheffler, H., & Elsässer, H., 1987, Physics of the Galaxy and Interstellar Medium, Springer-Verlag, Berlin

Schlegel, D.J., Finkbeiner, D.P., & Davis, M., 1998, ApJ, 500, 525

Schmidt, B.P., et al., 1998, ApJ, 507, 46

Schuster, W.J., & Nissen, P.E., 1989, A&A, 221, 65

Skillen, I., Fernley, J., Stobie, R.S., & Jameson, R.F., 1993, MNRAS 265, 301

Soderblom, D.R., King, J.R., Hanson, R.B., Jones, B.F., Fisher, D., Stauffer, J.R., & Pinsonneault, M.H., 1998, ApJ, 504, 192

Spitzer, L., 1978, Physical Processes in the Interstellar Medium, Wiley, New York

Stetson, P.B., & Harris, W.E., 1988, AJ, 96, 909

Storm, J., Carney, B. W., & Latham, D. W., 1994, A&A, 290, 443

Straniero, O., & Chieffi, A., 1991, ApJS, 76, 525

Straniero, O., Chieffi, A., & Limongi, M., 1997, ApJ 490, 425

Szabados, L., 1997, in HIPPARCOS Venice '97, ESA-SP 402, p. 657

Turner, M.S., 1997, Nucl. Phys. Proc. Suppl., 59, 239

Twarog, B.A., Anthony-Twarog, B., & Bricker, A.R., 1999, AJ, 117, 1816

Udalski, A., Szymański, M., Kaluzny, J., Kubiak, M., & Mateo, M., 1993, Acta Astron., 43,

Udalski. A., 1999, astro-ph/9910187

Udalski, A., Szymański, M., Kubiak, M., Pietrzyński, G., Woźniak, P., & Zebruń, K., 1998a, *Acta Astron.* 48, 1

Udalski, A., Pietrzyński, G., Woźniak, P., Szymański, M., Kubiak, M., & Zebruń, K., 1998b, *ApJ*, 509, 25

Tammann, G., 1998, in 21st Texas Symposium on Relativistic Astrophysics and Cosmology, in press

Tsujimoto, T., Miyamoto, M., & Yoshii, Y., 1998, *ApJ*, 492, L79

van Altena, Truen-liang Lee & Hoffleit 1995, The General Catalogue of Trigonometric Stellar Parallaxes (Yale University Observatory, New Haven)

van Leeuwen, F., Feast M. W., Whitelock, P. A. & Yudin, B. 1997, *MNRAS*, 287, 955

VandenBerg, D.A., 1998, IAU Symp. 189 on Fundamental Stellar Properties: the Interaction between Observations and Theory, eds. T.R. Bedding, A.J. Booth, J. Davis, Kluwer, Dordrecht, p. 439

VandenBerg, D.A., Bolte, M., & Stetson, P.B., 1990, *AJ*, 100, 445

VandenBerg, D.A., Bolte, M., & Stetson, P.B., 1996, *ARA&A*, 34, 461

Walker, A. R., 1992, *ApJ*, 390, L81

Wesselink, A.J., 1969, *MNRAS*, 144, 297

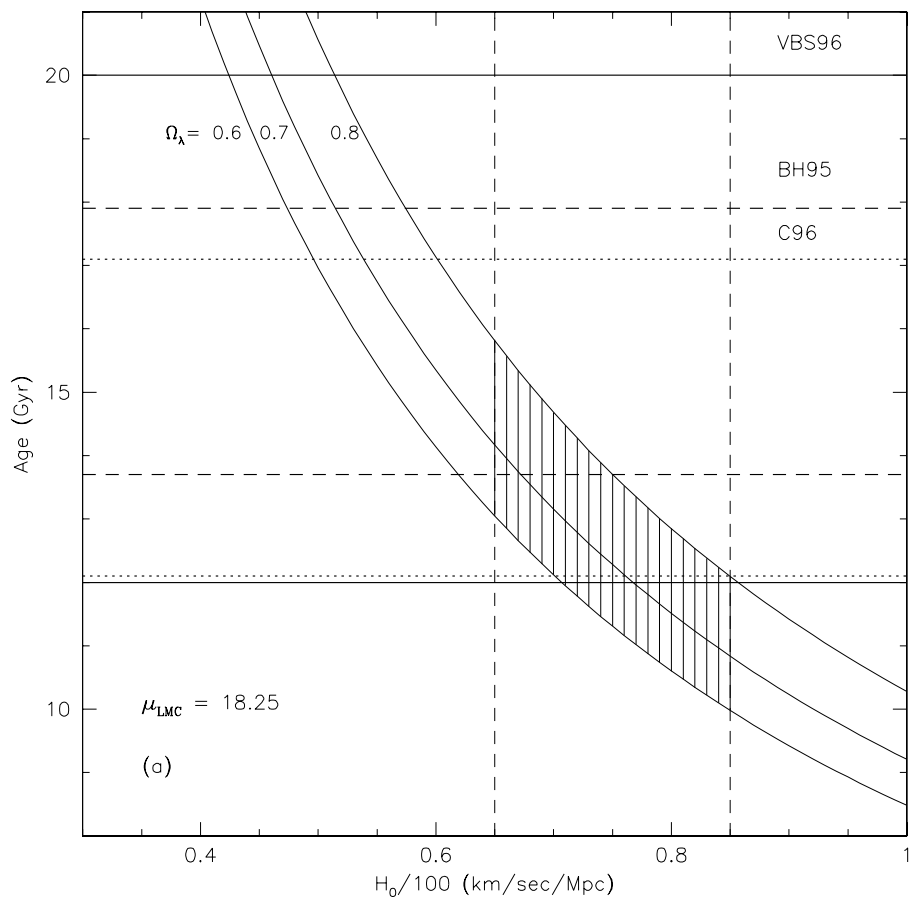
Zhao, G., & Magain, P., 1990, *A&A*, 238, 242

Zinn, R., 1980, *ApJS*, 42, 19

Zinn, R., & West, M.J., 1984, *ApJS*, 55, 45

Zoccali, et al., 1998, in STScI Symposium on Unsolved Problems in Stellar Evolution,

Baltimore, May 1998, M.Livio Ed., in press



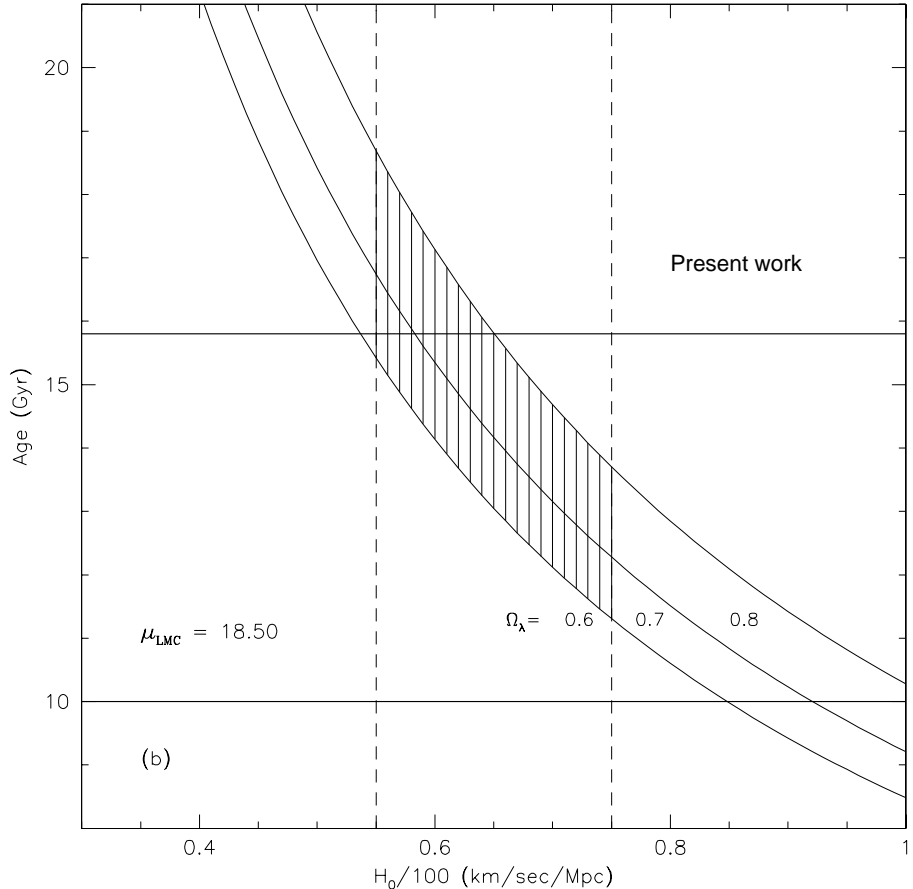


Fig. 1.— Age ( $t_0$ ) -  $H_0$  relationships, adapted from Turner (1997), for various cosmological models of flat-universe and for different values of  $\Omega_\Lambda = 1 - \Omega_m$ , with  $\Omega_m$  in the range suggested by recent type Ia SNe data ( $\Omega_m \sim 0.3 \pm 0.1$ ). The shaded area is the permitted region according to values of  $H_0$  consistent with the distance moduli used to derive ages for the globular clusters, before : panel (a) (Bolte & Hogan, 1995,  $t=15.8 \pm 2.1$  Gyr; Chaboyer et al., 1996,  $t=14.6 \pm 2.5$  Gyr; and VandenBerg, Bolte & Stetson, 1996,  $t=15^{+5}_{-3}$  Gyr.) and after : panel (b) the release of Hipparcos parallaxes.

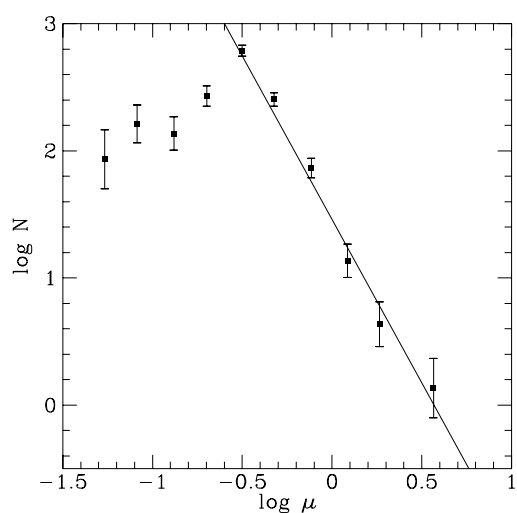


Fig. 2.— Proper motion distribution for stars in the present *a priori* sample.

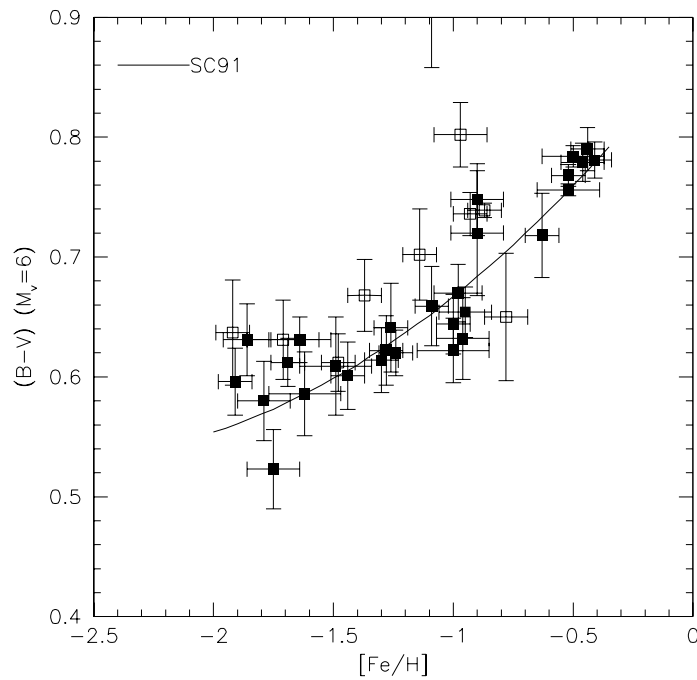


Fig. 3.— The  $(B-V)_{Mv=6}$ —[Fe/H] relation for stars in the *a priori* sample with  $\Delta\pi/\pi < 0.12$ . Filled symbols are *bona fide* single stars; open symbols are known or suspected binaries. Solid lines are the theoretical relations by Straniero & Chieffi (1991).

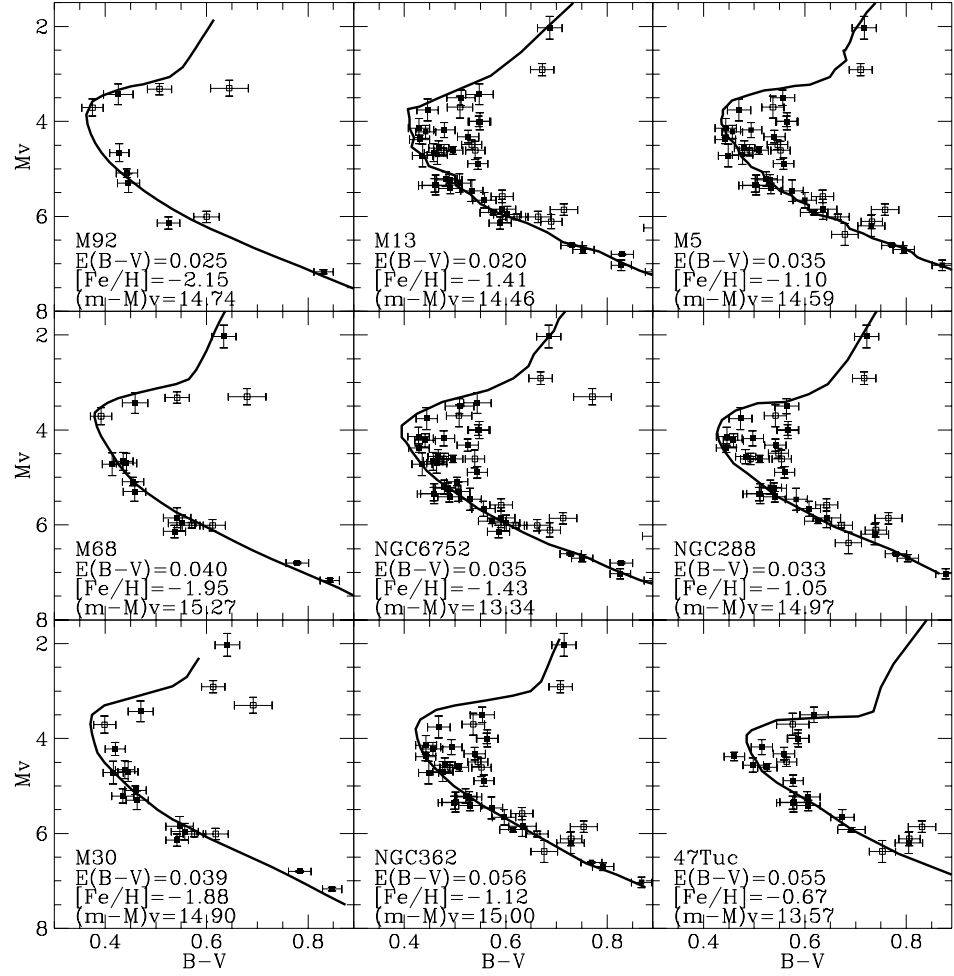


Fig. 4.— Fits of the fiducial mean loci of the Globular Clusters considered in this paper with the position of the subdwarfs. Only *bona fide* single stars with  $5 < M_V < 8$  mag are used in the fits (solid squares). The values of the parameters adopted in the present analysis are shown in each panel.

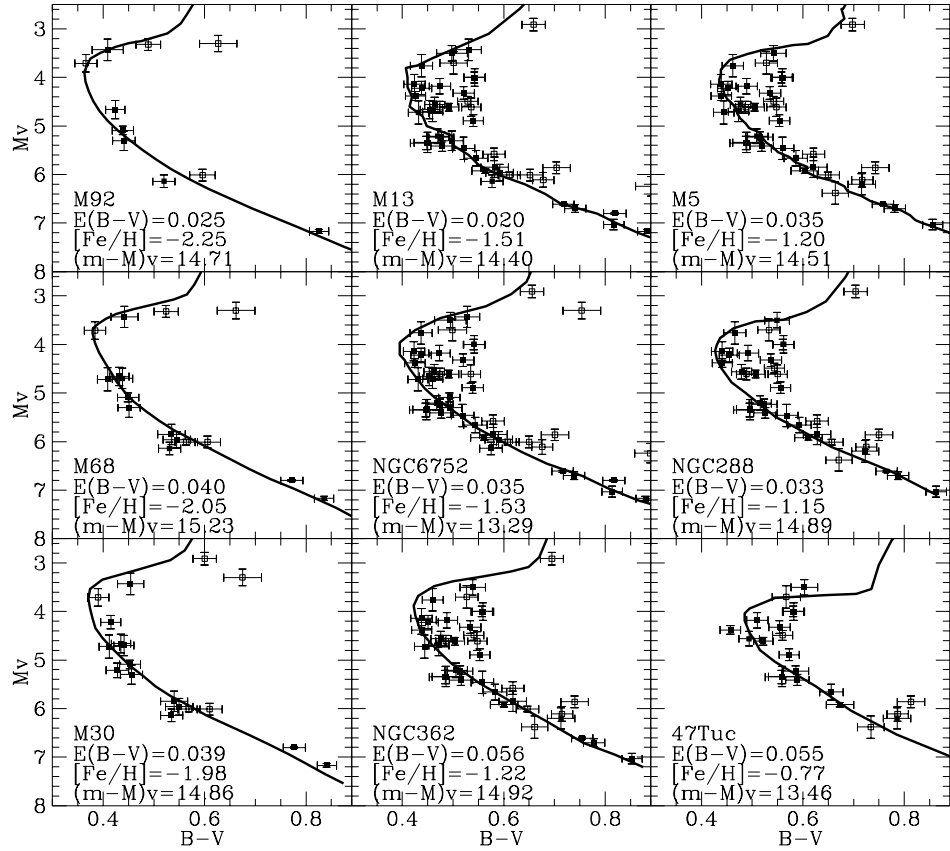


Fig. 5.— Same as in Figure 4, but assuming that metallicities of the globular clusters from Carretta & Gratton (1997) are systematically underestimate by 0.1 dex.

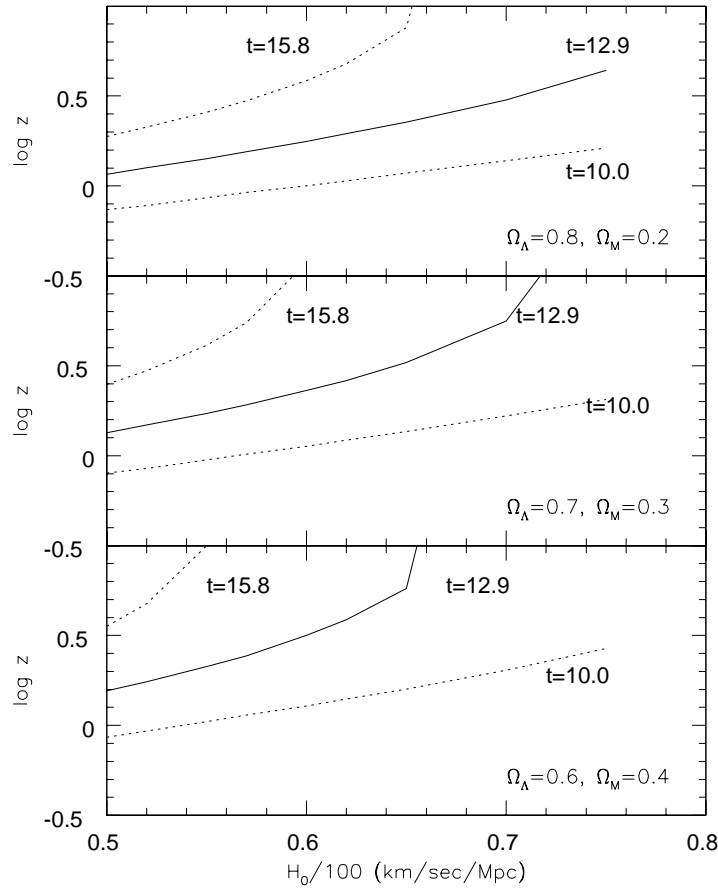


Fig. 6.— Epoch of formation of the galactic globular clusters against various possible values for the Hubble constant in a flat Universe  $\Omega_\Lambda = 1 - \Omega_m$ . The three panels correspond to 3 different values for  $\Omega_m$  (0.2, 0.3 and 0.4). The solid lines shows the favorite age of the globular clusters according to this paper (13.2 Gyr), the dashed lines represent the 95 % confidence level.

Table 1: Hipparcos-based distance moduli for globular clusters

NGC	Other	[Fe/H]	adopted	range	No.	$(m - M)_V$	$(m - M)_V$	cmd	Study
			$E(B - V)$		Stars	original	bin. corr.	source	
6341	M92	$-2.15a$	$0.025 \pm 0.005$	$-2.5 \div -1.5$	2	$14.82 \pm 0.08$	14.80	1	Paper I
		$-2.15a$	$0.025 \pm 0.005$	$-2.5 \div -1.5$	4	$14.74 \pm 0.07$	14.72	1	this paper
		$-2.20b$	0.02	$-2.6 \div -1.8$	17	$14.74 \pm 0.05$	14.67	1	PMTV
		$-2.24b$	0.02	$< -1.7$	10	$14.99 \pm 0.10$		1	R97
7078	M15	$-2.15a$	0.09	$< -1.7$	10	$15.66 \pm 0.10$		12,13	R97
4590	M68	$-1.95a$	$0.040 \pm 0.010$	$-2.5 \div -1.5$	2	$15.33 \pm 0.08$	15.31	2	Paper I
		$-1.95a$	$0.040 \pm 0.010$	$-2.5 \div -1.5$	7	$15.27 \pm 0.06$	15.25	2	this paper
		$-2.09b$	0.05	$< -1.7$	10	$15.45 \pm 0.10$		2	R97
7099	M30	$-1.88a$	$0.039 \pm 0.001$	$-2.5 \div -1.3$	3	$14.96 \pm 0.08$	14.94	3,4	Paper I
		$-1.88a$	$0.039 \pm 0.001$	$-2.5 \div -1.3$	8	$14.90 \pm 0.05$	14.88	3,4	this paper
		$-2.13b$	0.05	$< -1.7$	10	$15.11 \pm 0.10$		4	R97
6397		$-1.82a$	0.19	$-2.05 \div -1.5$	8	$12.83 \pm 0.15$		9	R98
6205	M13	$-1.41a$	$0.020 \pm 0.000$	$-1.8 \div -1.0$	9	$14.47 \pm 0.07$	14.45	5	Paper I
		$-1.41a$	$0.020 \pm 0.000$	$-1.8 \div -1.0$	17	$14.46 \pm 0.04$	14.44	5	this paper
		$-1.65b$	0.02	$-1.85 \div -1.4$	11	$14.54 \pm 0.10$		5,11	R97
		$-1.39a$	0.02	$-1.65 \div -1.15$	9	$14.51 \pm 0.15$		5,11	R98
		$-1.58$	0.02	$-1.76 \div -1.23$	7	$14.47 \pm 0.09$		5	C98
6752		$-1.43a$	$0.035 \pm 0.005$	$-1.8 \div -1.0$	9	$13.34 \pm 0.07$	13.32	6	Paper I
		$-1.43a$	$0.035 \pm 0.005$	$-1.8 \div -1.0$	18	$13.34 \pm 0.04$	13.32	6	this paper
		$-1.54b$	0.02	$-1.85 \div -1.4$	11	$13.23 \pm 0.10$		6a	R97
		$-1.42a$	0.04	$-1.27 \div -1.2$	12	$13.28 \pm 0.15$		6a	R98
		$-1.51$	0.04	$-1.76 \div -1.23$	7	$13.33 \pm 0.09$		6	C98
362		$-1.12a$	$0.056 \pm 0.003$	$-1.6 \div -0.8$	6	$15.06 \pm 0.08$	15.04	7	Paper I
		$-1.12a$	$0.056 \pm 0.003$	$-1.6 \div -0.8$	13	$15.00 \pm 0.05$	14.98	7	this paper
5904	M5	$-1.10a$	$0.035 \pm 0.005$	$-1.6 \div -0.8$	7	$14.62 \pm 0.07$	14.60	8	Paper I
		$-1.10a$	$0.035 \pm 0.005$	$-1.6 \div -0.8$	13	$14.59 \pm 0.05$	14.57	8	this paper
		$-1.40b$	0.03	$-1.6 \div -1.25$	8	$14.54 \pm 0.10$		8	R97
		$-1.10a$	0.02	$-1.35 \div -0.9$	9	$14.58 \pm 0.15$		8	R98
		$-1.17$	0.03	$-1.23 \div -1.07$	4	$14.51 \pm 0.09$		8	C98
		$-1.05a$	$0.033 \pm 0.007$	$-1.6 \div -0.8$	6	$14.96 \pm 0.08$	14.94	9	Paper I
288		$-1.05a$	$0.033 \pm 0.007$	$-1.6 \div -0.8$	12	$14.97 \pm 0.05$	14.95	9	this paper
		$-1.07a$	0.01	$-1.30 \div -0.85$	9	$15.03 \pm 0.15$		9	R98
		$-0.67a$	$0.055 \pm 0.007$	$-1.3 \div -0.5$	8	$13.64 \pm 0.08$	13.62	10	Paper I
104	47Tuc	$-0.67a$	$0.055 \pm 0.007$	$-1.3 \div -0.5$	7	$13.57 \pm 0.09$	13.55	10	this paper
		$-0.70a$	0.04	$-0.9 \div -0.45$	9	$13.68 \pm 0.15$		10	R98
		$-0.70a$	0.28	$-0.9 \div -0.45$	9	$14.06 \pm 0.15$		14	R98

References. — Metallicity sources: a. Carretta & Gratton (1997) b. Zinn & West (1984), and further updates.

CMD sources: 1. Stetson & Harris (1988) 2. McClure et al. (1987) 3. Bolte (1987b) 4. Richer, Fahlman & Vandenberg (1988)

5. Richer & Fahlman (1986) 6. Penny & Dickens (1986) corrected according to Vandenberg, Bolte & Stetson (1990) 7. Bolte

Table 2: Stars with  $\Delta\pi/\pi < 0.12$  in the *a priori* sample

HD	Gliese	$E(B - V)$	$V$	$\pi$	$\Delta\pi/\pi$	$M_V$	$\sigma_{M_V}$	$(B - V)_0$	$\sigma_{(B - V)_0}$	[Fe/H]	$\sigma_{[\text{Fe}/\text{H}]}$
-35 0360	G269-87	0.000	10.253	16.28	0.108	6.20	0.22	0.763	0.019	-0.90	0.11
6755	G243-63	0.030	7.632	7.74	0.118	1.94	0.24	0.680	0.019	-1.48	0.15
-61 0282		-0.000	10.109	11.63	0.102	5.34	0.21	0.526	0.019	-0.96	0.11
10607		0.010	8.298	14.00	0.053	4.00	0.11	0.562	0.020	-1.13	0.10
17072		-0.000	6.589	7.57	0.067	0.94	0.14	0.660	0.019	-1.34	0.15
19445	G037-26	0.002	8.045	25.85	0.044	5.09	0.09	0.458	0.020	-1.91	0.07
+66 0268	G246-38	0.000	9.916	17.58	0.087	6.07	0.18	0.652	0.020	-1.92	0.07
23439	G095-57A	0.000	7.828	40.83	0.055	5.86	0.12	0.778	0.019	-0.97	0.11
25704		0.000	8.118	19.02	0.046	4.49	0.10	0.553	0.020	-0.93	0.07
25329	Gl 158	0.000	8.502	54.14	0.020	7.17	0.04	0.864	0.018	-1.69	0.07
284248	G008-16	-0.008	9.257	12.84	0.104	4.70	0.21	0.458	0.020	-1.57	0.07
29907		0.000	9.883	17.00	0.058	6.01	0.12	0.632	0.020	-1.71	0.15
31128		0.010	9.095	15.57	0.077	5.00	0.16	0.480	0.020	-1.86	0.10
34328		0.003	9.436	14.55	0.069	5.21	0.15	0.478	0.020	-1.44	0.07
46663		0.010	9.514	21.80	0.110	6.09	0.23	0.927	0.020	-2.11	0.15
-33 3337		0.020	9.016	9.11	0.111	3.69	0.23	0.452	0.020	-1.33	0.07
64090	G090-25	0.000	8.276	35.29	0.029	6.01	0.06	0.614	0.020	-1.48	0.07
-80 0328	Gl 345	0.012	10.089	16.46	0.060	6.14	0.13	0.553	0.019	-1.75	0.11
84937	G043-03	0.009	8.300	12.44	0.085	3.71	0.18	0.382	0.020	-2.07	0.07
89499		0.010	8.609	8.93	0.082	3.30	0.17	0.687	0.020	-1.91	0.15
91345		0.010	9.016	17.70	0.053	5.23	0.11	0.550	0.018	-0.98	0.10
94028	G058-25	-0.000	8.221	19.23	0.059	4.61	0.12	0.482	0.020	-1.32	0.07
97320		0.010	8.145	17.78	0.043	4.39	0.09	0.447	0.020	-1.01	0.10
102200		0.001	8.751	12.45	0.096	4.14	0.20	0.438	0.020	-1.22	0.15
+51 1696	G176-53	0.000	9.913	13.61	0.113	5.46	0.23	0.552	0.020	-1.26	0.07
103095	G122-51	0.000	6.422	109.21	0.007	6.61	0.02	0.752	0.019	-1.24	0.07
108177	G013-35	0.002	9.662	10.95	0.118	4.72	0.24	0.430	0.020	-1.55	0.07
111980		0.010	8.338	12.48	0.111	3.70	0.23	0.532	0.020	-1.16	0.11
113083		0.010	8.014	18.51	0.061	4.32	0.13	0.540	0.020	-1.09	0.11
116064		0.010	8.780	15.54	0.093	4.66	0.19	0.440	0.019	-1.86	0.07
120559		0.020	7.918	40.02	0.025	5.92	0.05	0.642	0.019	-0.95	0.11
121004		0.010	8.999	16.73	0.081	5.06	0.17	0.606	0.020	-0.90	0.11

Table 2.

*continued*

HD	Gliese	$E(B - V)$	$V$	$\pi$	$\Delta\pi/\pi$	$M_V$	$\sigma_{M_V}$	$(B - V)_0$	$\sigma_{(B - V)_0}$	[Fe/H]	$\sigma_{[\text{Fe}/\text{H}]}$
126681		-0.001	9.302	19.16	0.075	5.66	0.16	0.602	0.020	-1.09	0.07
132475		0.037	8.439	10.85	0.105	3.51	0.22	0.522	0.020	-1.73	0.09
134440		0.005	9.418	33.68	0.050	7.03	0.11	0.845	0.018	-1.28	0.07
134439		0.005	9.052	34.14	0.040	6.70	0.08	0.767	0.019	-1.30	0.07
140283	GJ1195	0.024	7.137	17.44	0.056	3.32	0.12	0.463	0.019	-2.40	0.07
145417		0.010	7.496	72.75	0.011	6.80	0.02	0.805	0.019	-1.64	0.11
149414A	G017-25	0.010	9.581	20.71	0.072	6.11	0.15	0.726	0.018	-1.14	0.07
159482	G139-48	0.020	8.320	20.89	0.056	4.89	0.12	0.560	0.020	-1.06	0.10
+05 3640	G140-46	0.010	10.350	17.00	0.112	6.38	0.23	0.732	0.020	-0.78	0.09
166913		0.010	8.191	16.09	0.065	4.18	0.14	0.441	0.020	-1.44	0.07
188510	G143-17	0.001	8.830	22.80	0.061	5.58	0.13	0.598	0.020	-1.37	0.07
189558		0.010	7.703	14.76	0.075	3.50	0.16	0.565	0.020	-1.04	0.10
+42 3607	G125-64	0.040	9.986	12.02	0.094	5.30	0.20	0.470	0.020	-1.79	0.11
193901		0.003	8.644	22.88	0.054	5.41	0.11	0.549	0.020	-1.00	0.07
194598	G024-15	0.003	8.335	17.94	0.069	4.56	0.15	0.484	0.020	-1.02	0.07
196892		0.001	8.244	15.78	0.077	4.18	0.16	0.497	0.020	-1.04	0.15
+41 3931	G212-07	0.030	10.182	14.24	0.103	5.85	0.21	0.584	0.020	-1.49	0.15
201891		0.003	7.367	28.26	0.036	4.61	0.08	0.514	0.019	-0.97	0.07
204155	G025-29	0.000	8.492	13.00	0.085	4.00	0.18	0.571	0.020	-0.98	0.10
-00 4234	G026-09	0.010	9.765	20.26	0.099	6.21	0.20	0.947	0.019	-1.09	0.15
205650		-0.000	9.044	18.61	0.066	5.35	0.14	0.518	0.020	-1.00	0.15
+59 2407	G231-52	0.050	10.115	15.20	0.080	5.96	0.17	0.580	0.021	-1.62	0.15
211998		0.010	5.280	34.60	0.060	2.91	0.13	0.669	0.020	-1.43	0.10
219175A	G157-32	0.000	7.570	26.52	0.091	4.61	0.19	0.544	0.018	-1.31	0.15

Table 3: Revised distances and ages for the 9 programme globular clusters

Cluster	Stars	$(m - M)_V$	$(m - M)_V$	$M_V(\text{HB})$	$M_V(\text{TO})$	Age (Gyr)
		original	bin cor.			
M92	4	$14.74 \pm 0.07$	14.72	$0.33 \pm 0.10$	3.98	14.8
M68	7	$15.27 \pm 0.06$	15.25	$0.46 \pm 0.11$	3.85	12.3
M30	8	$14.90 \pm 0.05$	14.88	$0.32 \pm 0.13$	3.85	12.3
M13	17	$14.46 \pm 0.04$	14.44	$0.51 \pm 0.17$	4.06	12.6
N6752	18	$13.34 \pm 0.04$	13.32	$0.43 \pm 0.17$	4.08	12.9
N362	13	$15.00 \pm 0.05$	14.98	$0.45 \pm 0.13$	3.87	9.9
M5	13	$14.59 \pm 0.05$	14.57	$0.54 \pm 0.09$	4.03	11.2
N288	12	$14.97 \pm 0.05$	14.95	$0.45 \pm 0.13$	4.05	11.2
47Tuc	7	$13.57 \pm 0.09$	13.55	$0.55 \pm 0.17$	4.20	12.5

Table 4: Systematic effects and total error budget associated with the MS fitting distances to GCs

Effect	$\Delta(m - M)$
Malmquist bias	negligible
Lutz-Kelker	$\pm 0.02$
Metallicity bias	only <i>a posteriori</i> sample
Binaries (in the field)	$\pm 0.02$
Binaries (in clusters)	$\pm 0.03$
Non solar abundance ratios	negligible
Photometric calibrations	$\pm 0.04$
Reddening scale	$\pm 0.07$
Metallicity scale	$\pm 0.08$
Total uncertainty ( $1\sigma$ )	$\pm 0.12$

Table 5: Sources of errors in Cluster age determination

Error source	Distribution	$\sigma$	Limits
		(Gyr)	(Gyr)
Internal	gaussian	0.5	
Lutz-Kelker	gaussian	0.25	
Binaries	gaussian	0.25	
Metallicity	flat		-1,+1
$[\alpha/\text{Fe}]$	flat		-0.3,0.8
Reddening	gaussian	0.9	
Color calibration	gaussian	0.5	
Convection	flat		-0.4,0.4
Code	flat		-0.4,0.4
Diffusion	flat		-1.0,0
Solar $M_v$	flat		-0.3,0.3

Table 6: True distance modulus to the LMC according to various methods

Population I	
Cepheids: Trig. parallaxes	$18.70 \pm 0.16$
Cepheids: MS fitting	$18.55 \pm 0.08$
Cepheids: Baade-Wesselink	$18.55 \pm 0.10$
Eclipsing Binaries	$18.30 \pm 0.07$
Red clump	?
Miras	$18.54 \pm 0.18$
SN1987a	$18.58 \pm 0.05$

Population II	
Subdwarf fitting	$18.64 \pm 0.12$
HB Trig. parallaxes	$18.50 \pm 0.11$
RR Lyr: Stat. parallaxes	$18.38 \pm 0.12$
RR Lyr: Baade-Wesselink	$18.40 \pm 0.2$
RR Lyr: Double mode	$18.47 \pm 0.19$
GC Dynamical models	$18.50 \pm 0.11$
WD cooling sequence	$18.4 \pm 0.15$